Design, Fabrication, and Operational Parameters of a Supercritical Water Oxidation Reactor

Stuart J. Moore

A thesis

submitted in partial fulfillment of the

requirements for the degree of

Master of Science

University of Washington

2020

Committee:

Igor Novosselov, Chair

John Kramlich

Per Reinhall

Program Authorized to Offer Degree:

Mechanical Engineering

University of Washington

Abstract

Design, Fabrication, and Operational Parameters of a Supercritical Water Oxidation Reactor

Stuart J. Moore

Chair of the Supervisory Committee:
Igor V. Novosselov
Department of Mechanical Engineering

Supercritical Water Oxidation (SCWO) has been shown to efficiently destroy wet organic wastes. The process, iterations, and lessons learned during the design and fabrication process of a continuous, inverted SCWO reactor are described. Ethanol is oxidized in a continuous inverted supercritical water oxidation reactor at 25 MPa, with oxidant and fuel preheat temperatures of 380 to 450 °C. Optimal conditions for future operation are found by operating at various premixed fuel concentrations of 0-7 mol% ethanol in water, varying the air to fuel equivalence ratio from 1.1 to 1.8, and utilizing air and hydrogen peroxide as the oxidant. Experimental conditions are chosen for analysis of reactor temperatures during complete oxidation of pilot fuel, where ethanol will rapidly oxidize. Higher premixed concentrations of ethanol produce a more localized, higher temperature reaction occurring closer to the nozzle with longer residence times. Preliminary results find the use of air results in lower reaction temperatures than hydrogen peroxide at similar operational conditions due to nitrogen loading; the experiments with air are still on-going. The results are used to determine the capability of the reactor for the destruction of toxic organic compounds.

TABLE OF CONTENTS:

TABLE OF FIGURES:

ACKNOWLEDGEMENTS:

This research was possible by the funding provided by DTRA. Additional resources available to me from the University of Washington and within the Novosselov Research Group contributed immensely to my research as well.

I would like to thank my advisor, Prof. Igor Novosselov for his continued support and guidance over the last two years. His confidence in my abilities and encouragement has been exceptional. Additionally, I would like to thank my committee members Prof. Per Reinhall and Prof. John Kramlich for their advice and insight during this time.

I would also like to thank Elizabeth Rasmussen for her mentorship and advice as well as Brian Pinkard, Byron Ockerman, John Misquith, Anmol Purohit, Tim Wallace and the rest of the supercritical team for there particular areas of expertise and assistance in the completion of the SCWO Reactor. Additionally, thank you to the rest of their lab for putting up with my random questions and many naps.

I'm thankful for the many friends I made during my time here at UW. And of course, a big thank you to my roommates, Abigale Snortland and Michael Rauenbuehler, and all my other friends. A larger thank you to my family for their support in my continued education. Oh, last but not least, thanks Stacy - Love you all.

1. INTRODUCTION

1.1 The Problem and Proposed Solution

Waste management is currently one of the world's most pressing environmental issues as the production of waste continues to increase and is projected to grow [1]. Land scarcity and ethics are demanding solutions other than plastic islands, growing landfills, and high-emission facilities for proper disposal of the current gamut of humanmade organic waste. A process known as supercritical water oxidation (SCWO) has been shown to destroy sewage sludge [2-7], industrial wastes [8-11], plastics [12-19], and other municipal solid wastes (MSW) [20, 21]. The advantages of SCWO for the destruction of MSW is the conversion of almost all wastes to CO_2, H_2O, and N_2 with no harmful emissions of NO_X, SO_2, or particulate matter [22]. Metals and minerals not combusted during the process can be filtered out as a slurry or solid waste, and if required, a water treatment step can render the water discharge as clean [23]. SCWO has been promising in destroying exceptionally toxic and dangerous wastes such as chemical warfare agents (CWA's) [24, 25]. Most of CWA's remaining in the US are currently stockpiled in military holding facilities awaiting destruction. The destruction of wet-hazardous waste such as CWAs is a time pressing issue concerning degradation, pollution, and environmental and human safety. SCWO has no harmful emissions and is optimized for use with wet wastes, mitigating the need for additional energy spent drying as used in current means of destruction, incineration [26]. There are still many tons of stockpiled CWA's waiting to be destroyed, but according to S.2182 – National Defense Authorization Act for Fiscal Year 1995, Public Law No: 103-337, transportation of CWA's is no longer permissible across state lines within the US [27]. This requires destruction facilities built at the location of the stockpile. The US is not the only country with CWA's awaiting destruction. Therefore, the need for a small scale, mobile SCWO system is desired and does not currently exist commercially.

Supercritical water (SCW) is a convenient reaction medium for the destruction of organic, wet wastes. The critical point of fluid exists at a defined pressure and temperature. Past its critical point, the fluid is known to be a supercritical fluid. Supercritical fluids are one phase but cannot be explicitly defined as a liquid or gas as they exhibit properties of both. SCW occurs above the critical point (374°C, 22.1 MPa). At supercritical conditions, properties of water change drastically, exhibiting a low dielectric constant, density, and disassociation constant [26], some of which can be observed in Figure 1. Supercritical water

gasification (SCWG) reactors work via hydrolysis, where beyond the critical point, water becomes a non-polar solvent in which organic molecules are completely miscible and breakdown.

Oxygen is completely miscible in SCW, [28] creating a homogeneous mixture with desirable transport properties. These properties of SCW make it an ideal reaction medium for oxidation to occur [29]. The addition of an oxidant such as oxygen, air, or hydrogen peroxide causes a reaction is known as supercritical water oxidation (SCWO). SCWO's main advantage is its high reaction density compared to that of incineration, which allows for operation at a cooler temperature (almost half of the incineration temperatures) with residence times remaining less than a minute. This leads to cleaner products that are free of CO, NO_X, SO_2, and dioxins [22].

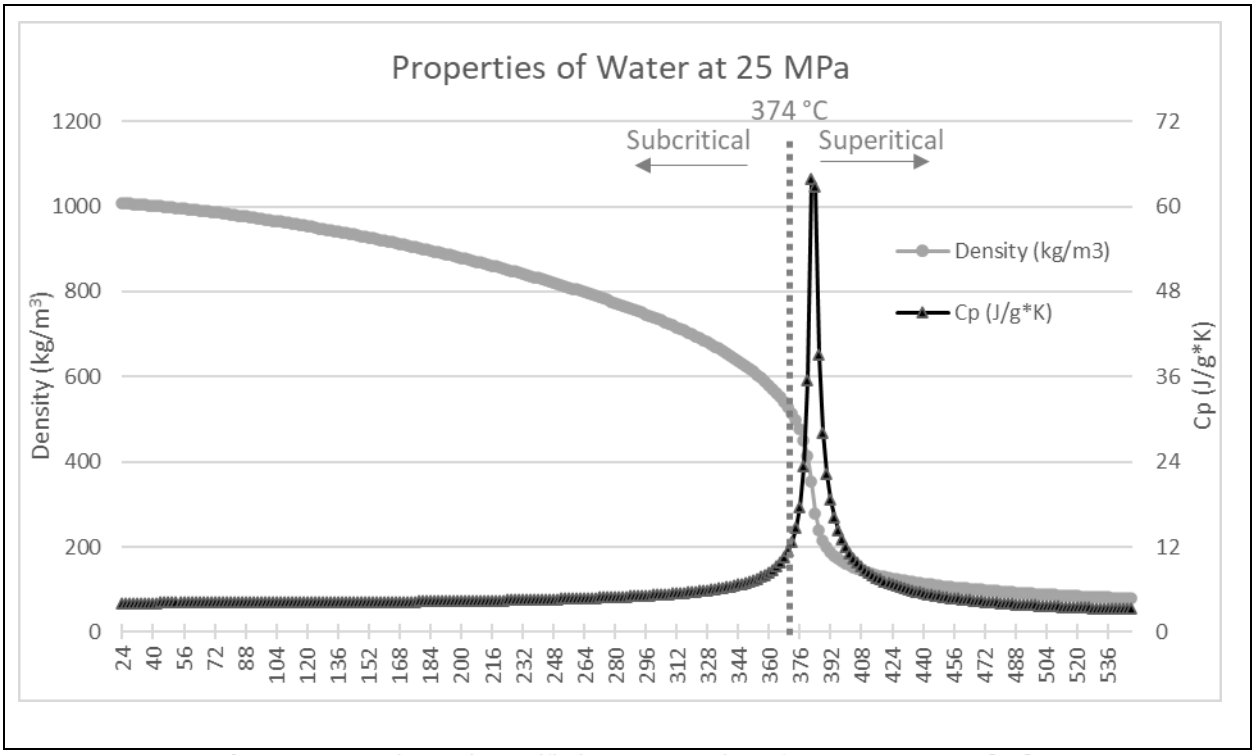

Figure 1: Density and specific heat properties of water at 25MPa [30].

A lab-scale, continuous SCWG reactor that was designed and built at the University of Washington [31] was used to study reaction kinetics of simple model compounds in subcritical and supercritical water. While this reactor is capable of destruction of simple compounds such as ethanol or isopropanol, it cannot handle the more complex feedstocks with a high salt or heteroatom contents found in CWA's or CWA surrogates such as dimethyl methylphosphonate (DMMP). The reaction of more complex compounds such as DMMP

may produce inorganic precipitates, such as phosphorous, which are insoluble in SCW and lead to eventual plugging of the reactor. Additionally, the SCWG reaction is endothermic and requires an external heat source to sustain the process, creating an overall costly operation. Like SCWG, SCWO is a viable option in the destruction of toxic organic wastes [31]. Due to the exothermic reaction associated with SCWO, less external heat is needed to sustain the reaction.

1.2 Scope of the Thesis

This thesis focuses on the design, fabrication, and testing of a bench-scale SCWO reactor intended to destroy CWA's and CWA surrogates while mitigating issues that have been problems in previous reactors. Previous reactors have used air [26, 32-35], H_2O_2 [25, 36], or pure oxygen [29, 35, 37] as oxidants. The reactor was constructed for operation with both air and H_2O_2 as oxidants to study. The use of pure oxygen was not explored as it was deemed to be too dangerous, posing an unnecessary risk. By allowing the flexibility and operation with both air and H_2O_2 as oxidants, testing, and comparison of multiple conditions and configurations require no additional cost for finding optimal operational conditions. The modular reactor design also allows for the replacement of parts as corrosion and plugging issues arise. The work aims to understand and characterize the reactor operation on a simple pilot fuel at varied concentrations and oxidant sources by measuring system response and behavior. The data can be used for validating CFD models and future operations with more complex feedstocks such as CWA and other toxic waste.

Complimentary efforts in SCWO reactor modeling and control associated with the design and fabrication of this reactor were simultaneously performed but are out of the scope of this thesis. Additionally, testing of various configurations of the reactor past the initial operational configuration as well as CWA surrogates are also out of the scope of this thesis and will be considered in future work.

2. REVIEW OF SUPERCRITICAL WATER OXIDATION REACTORS

2.1 History and Background of Supercritical Water Oxidation Reactors

The state of the art for industrial-scale destruction of toxic waste is either incineration or wet oxidation. During incineration, toxic waste is burned at high temperatures (900-1100°C). Incineration is best used for low H_2O concentration waste because high moisture content leads to low flame temperatures and poor waste destruction efficiency. For aqueous wastes, wet oxidation is a more efficient option and occurs below the supercritical region between 200-300°C, 4.1-13.8 MPa. This typically requires residence times of 30 or more minutes to fully decompose a given agent, most typically organic wet waste [26]. Even after these long residence times, full decomposition may still not occur for some wastes. During the wet oxidation process, the solubility of oxygen is less than the amount necessary for complete combustion. This process of incomplete combustion yields non-desirable byproducts that require further treatment [26].

SCWO reactors have been progressively developed since Modell patented the first reactor in 1982 [38]. It was initially developed as an alternative to wet-oxidation and incineration for toxic aqueous waste. Research focusing on SCWO reactors has continued since the early 1980's due to promises of low environmental impact, low energy use, cost, and treatment success. Temperatures required for rapid and complete oxidation of organics in SCWO (450-600°C) are nearly half of that needed for incineration in air at similar residence times [3]. Compared to wet-oxidation and incineration, under the right operating conditions, SCWO has been shown to burn cleaner, eliminating NO_X, SO_2, and CO emissions [22, 39]. Even after 40 years of research, SCWO has not yet become an industry-standard due to engineering challenges such as corrosion, salt plugging, and operational costs.

2.2 Challenges

2.2.1 Corrosion

Within the SCWO reactor, there are typically two specific corrosion regimes: when the fluid temperature in the reactor is subcritical ($T < T_C$) where high solubility of corrosion products causes rapid corrosion, and $T > T_C$ where extremely oxidative conditions cause corrosion. General corrosion, pitting corrosion, and stress

corrosion cracking are the most likely to be observed. General corrosion is common and occurs uniformly over the exposed surface. During operation, an oxide layer is expected to form on the reactor walls leading to general corrosion. However, this oxide layer can be beneficial in decreasing the amount of pitting corrosion, which is more aggressive and detrimental than general corrosion from the oxide layer itself. Pitting corrosion is associated with penetration of an aggressive element or compound into a local region of the oxide layer. In the case of stainless steels and most alloys, at intermediate temperatures (>~200C), the oxide layer is weakened by the heat, leading to more aggressive pitting. Pitting is dangerous as a failure of fittings or tubing cannot be easily predicted. At high temperatures, above the inversion temperature (~200C), pitting rates do not decrease but resemble that of general corrosion. Although the corrosion rate does not decrease, general corrosion is a more linear degradation and, therefore, can be predicted [40]. The choice of materials can be utilized to mitigate the rate of corrosion due to pitting; however, feedstocks will determine which materials are best suited for mitigation [22]. As the reactor is typically operated and maintained at temperatures well above the inversion point, pitting corrosion is likely the dominant process and should be able to be predicted, except, perhaps in the heat exchanger.

Even without the effects of pitting corrosion, detrimental failure can still arise from stress corrosion cracking (SCC). Due to the extreme pressure and temperatures of the reactor, the reactor materials, most commonly Hastelloy C-276, Titanium, and Inconel 625 [31] are under considerable stress. The ultimate tensile strength (UTC) of these materials in high-temperature water in the presence of hydrogen or oxygen (both present during SCWO operation) decreases due to the presence of SCC [40]. In a particular case study, Shen [41] reports that as the temperature increases, the effect of SCC in the presence of SCW and sc-wet air on the ultimate tensile strength (316Ti SS) decreases (significantly for temperatures above 550°C). This is not to say, however, that the UTS of the material does not still decrease due to temperature effects. Because SCWO reactors experience heat cycles, it is possible to spend time in an operating regime below 550°C where effects due to SCC are important and left unchecked over time can result in an unpredictable failure.

To conclude, corrosion rates are typically highest for high-temperature, high-density fluids. Subsequently, lowest corrosion rates are found at the highest operating temperatures within the supercritical region (well past the critical point) of the SCWO reactor, where density is the lowest. It is important to note that while some materials are better suited to mitigate corrosion from certain species, there is no one best material,

and corrosion rates will depend on the feedstock. A combination of material types for various sections of the reactor is utilized in most reactors to prevent corrosion. Preventing corrosion altogether for all feedstocks with current material limitations is unfortunately not feasible.

2.2.2 Salt Precipitation and Clogging

As water transitions to supercritical water, the polarity of the water changes. This change in polarity leads to a change in solubility in which inorganics, such as salts, are no longer soluble. Instead, these salts that may exist as solids in the waste or form as a product of the reaction, precipitate on the walls. The eventual buildup can lead to plugging if not mitigated. Previous reactors have attempted to solve this problem in various ways, from chemical additives [42, 43], liners [24, 44-46], mechanical stirrers/scrappers [45], cooled walls [34, 47, 48], transpiring walls [35, 37, 49, 50], and combinations of these. The formation of char and tar within the reactor may occur depending on operational conditions [2]. Char and soot forms when running the reactor fuel-rich [51], which also can lead to plugging. Plugging of the reactor will lead to an increase in pressure and will eventually lead to failure of the continuous reactor.

2.2.3 High Operational Costs

Other technologies, such as incineration, can utilize energy recovery during operation. This process reduces the impact on energy use and reduces the cost of operation. To make the SCWO process economically viable, energy recovery methods are needed. Use of SCWO over SCWG already reduces the energy cost of the system as the oxidation reaction is exothermic; however, additional energy harvesting will further reduce costs. This becomes an issue with the reactor scale-up. This issue is explored in the literature [3, 11, 52], and it is not the scope of this report.

3. DESIGN 1

3.1. Design Concept

The UW SCWO system was designed based upon reactors built in the NRG lab and the reactors found in the literature [24, 29, 32, 33, 46]. The reactor design focused on mitigating potential plugging issues while retaining a small enough footprint for system mobility. Steps taken in plugging mitigation were hypothesized to help with corrosion; however, no drastic measures were employed other than material selection to minimize this issue. High operational costs were not a current concern and, if needed, can be addressed in future work.

When complex heteroatomic molecules were run through the previous SCWG (hydrolysis) reactor, the reactor plugged due to the buildup of insoluble inorganic precipitates on the reactor walls. Plugging also occurred during partial oxidation of ethanol due to soot build up [51]. The issue was compounded by the small inner diameter of the reactor section chosen to obtain the plug flow region for chemical kinetic studies.

An inverted hydrothermal flame design with a 0.5” ID reactor section was proposed to eliminate the fouling associated with more complex compounds seen in the previous SCWG reactor. The reactor was inverted to produce desired recirculation effects due to buoyancy, resulting in longer residence times within the flame for the complete destruction of waste compounds. To address the issue of fouling, the use of a novel sheath flow of water around the flame was hypothesized to act as both quench water for the system and prevent the deposit of precipitates on the reactor walls. The design was intended to be “mobile”, so the entire reactor fits inside a laboratory fume hood no larger than 4’ x 2’ x 3.5’ (LxWxH).

3.1.1 Tubing, Fittings, and Material Selection

The reactor is comprised of high-pressure stainless steel 316 (AISI 316 or SS 316) tubing in the low-temperature regions and high-pressure Inconel 625 tubing in the high-temperature regions. Inconel 625 was chosen for its excellent resistance to oxidation and most corrosive species. While SS316 has a higher melting point, it has a lower ultimate tensile and yield strength as well as a lower operating temperature (870°C) than Inconel 625 and significantly lower tensile strength at this operating temperature. Iron-based alloys were also found to corrode faster than Nickle based alloys in SCW and in the presence of corrosives. SS316 was used instead of SS304 as the addition of molybdenum in SS316 makes it considerably more

resistant to chemical corrosion (especially due to salts) and oxidation at higher temperatures. Corrosion has been studied extensively and is outlined well by Marrone and Hong [22]. Due to material selection, safe operation can occur at reactor wall temperatures <650°C. Most fittings in the reactor were purchased from High-Pressure Equipment Co. In the case of a blockage, rupture disks rated to 5500psi were placed before the reactor section and in line with all pumps as seen in Figure 2. Fittings label as “Custom” in Figure 2 consist of modified fittings purchased from High-Pressure Equipment. These alterations were needed for the custom co-flow nozzle, further described in Section 3.1.2, to end within the reaction chamber. At the thermocouple locations, the internal fitting diameters were increased to insert the 3.175 mm Inconel thermocouples directly into the flow for accurate fluid temperature measurements. A replaceable titanium liner is inserted to increase the reactor section’s resistance to corrosion and fouling.

3.1.2 Reactor Section

The reactor section consists of two main components: the co-flow nozzle and the reaction chamber. The co-flow nozzle consists of two concentric tubes, the inner transporting wet fuel and the outer, a wet oxidant for the formation of a diffusion flame. In this first reactor design, the inner fuel line is 3.175 mm (1/8”) OD Inconel 625 tube with an internal cross-sectional area of 2.45 mm^2 (0.0038 in^2). The outer oxidant line is 9.525 mm (3/8”) OD Inconel 625 tube with an internal cross-sectional area of 22.52 mm^2 (0.0349 in^2). The primary factor for choosing a 9.525mm tube with a significantly larger area is because the 6.35 mm (1/4") OD high-pressure tubes’ ID is 3.05mm (0.12”) (<3.175 mm). The nozzle was manufactured such that the end of the concentric tubes are flush with one another. The reactor section has an internal volume approximately 1120mL and is comprised of 19.05 mm (3/4”) OD, SS 316 (t = 6.35 mm (1/4")) lined with a 12.7 mm (1/2”) OD (t= 0.89 mm (0.035”)) replaceable titanium liner. The removable titanium liner provided a temperature and corrosion barrier for extended reactor life. A copper coiled heat exchanger wrapped around the reactor section provides additional wall cooling (6.35 mm OD copper tubing). The heat exchanger coil is connected to a 2kW ALX-2000-P400 Koolance cooling system. The original design called for a thermowell to measure flame temperature due to its durability over a thermocouple; however, no thermowells were found to fit this design. Instead, a 3.175 mm K-type Inconel 625 thermocouple (TC) from OMEGA is inserted from the opposite (from the nozzle) end of the reactor section. It extended vertically in line with the nozzle, and the position can be adjusted by the length of the thermocouple, represented by

“Reactor Section TC” in Figure 2. Not only did the flame front have the potential to be hotter than the operating conditions of the TC, but Hicks reported that objects located too close to the nozzle would affect the autoignition parameters of the flame [33]. As the reactor section was built without a sapphire window to observe flame position, reliance on previously reported studies [29, 32, 33] and thermocouple readings were important for understanding the dynamics of the internal system. Even though it is not possible to obtain the exact flame temperature in this system, it would attempt to determine flame stability by analyzing temperature fluctuations reported by the downstream thermocouple. Insulation and heating tape ensure heat loss is reduced. Finally, a TC located downstream of the reactor section makes sure the heat exchanger adequately cools the flow for safe use with the back-pressure regulator (BPR) (rated to 70°C). A schematic of the reactor section and TC locations can be found in Figure 2, and the reactor section schematic in Figure 3.

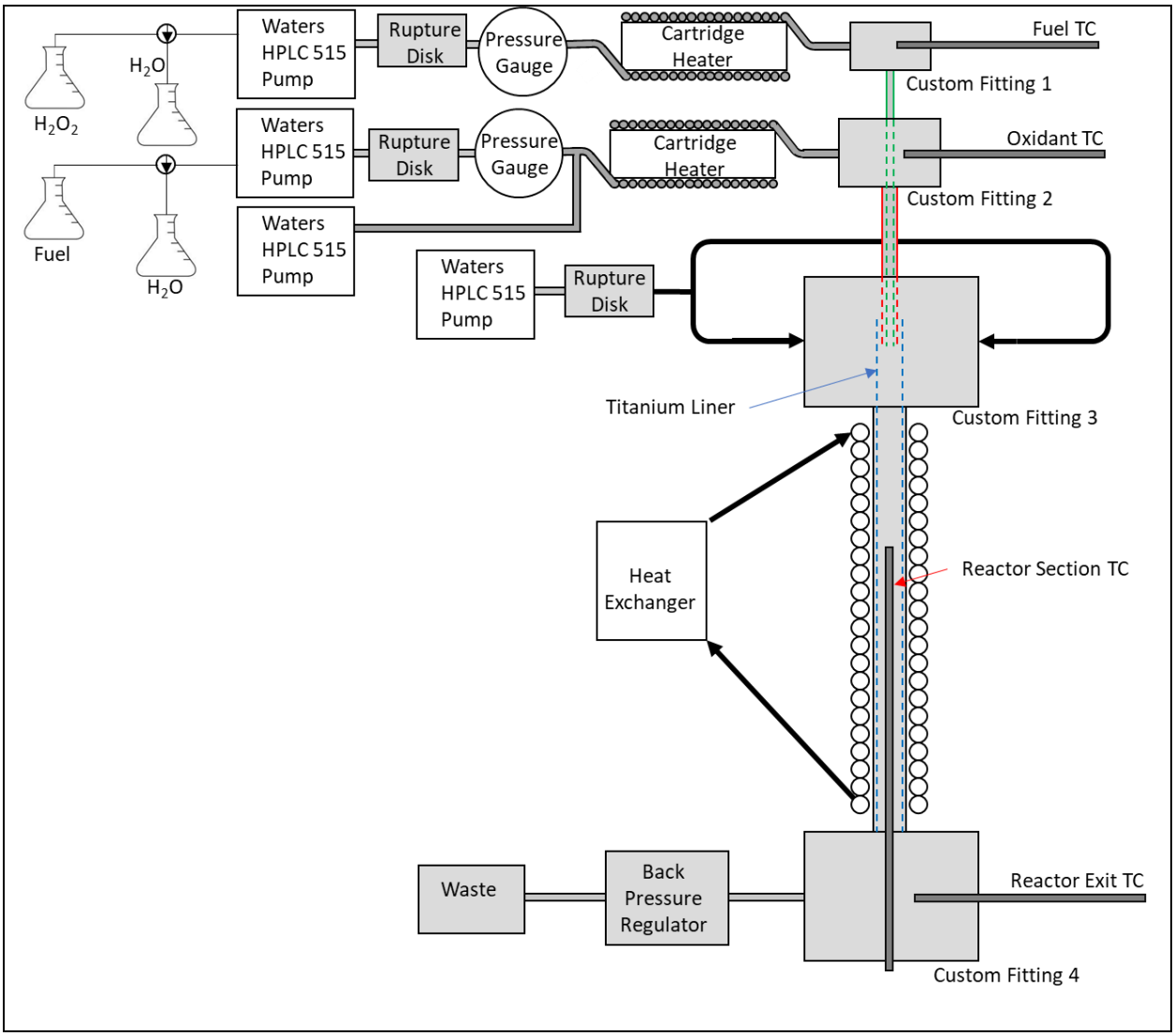

Figure 2: Design 1 reactor schematic, with hydrogen peroxide as oxidant.

3.1.3 Pump Selection and Pressure Generation

High-Pressure Liquid Chromatography (HPLC) pumps are common in SCW systems (SCWG and SCWO) and worked well in the NRG UW SCWG reactor [31]. Waters 515 HPLC pumps are initially used this reactor as they are capable of flow rates of 10 mL/min with a maximum operating pressure of 41.3 MPa, well above the operating pressure of the reactor (25MPa). Furthermore, these pumps have a “high-pressure” setting in which the pump can be set to automatically shut off in case of plugging. Four HPLC pumps control the flow rate of the fuel, oxidant, and sheath flow. After the initial study and confirmation of autoignition, the addition of a LEWA diaphragm pump would control the sheath flow of water. This diaphragm pump was chosen as it is capable of flow rates of 225 mL/min at 25MPa. This larger flow rate was the driving factor in

the pump selection because operation for extended periods with flame temperatures of ~2000K will likely require higher sheath flow rates to adequately cool the reactor. The LEWA pump would later be used for controlling the flow rate of a reagent into the system.

3.1.4 Heater Subsystem

To heat water from ambient to 400°C with a constant pressure of 25 MPa, roughly 2450 kJ/kg of heat must be transferred to the fluid. For flow rates of 10 mL/min, 415 W is needed. As observed in previous reactors [33, 53], and summarized by Gorman [31], tubing coiled around a cartridge heater works well to heat a fluid past the critical point. To account for the heating of different liquids and to achieve higher temperatures, 1 kW cartridge heaters were selected for the oxidant and the fuel streams. Each heater is controlled using OMEGA Platinum PID temperature controllers mounted to the lower front panel for ease of use. These PID controllers are controlled with a computer via a micro-USB port.

Since the cartridge heaters did not have an internal TC, a 1/16” K-type Inconel 625 TC, located between the heater and coiled tubing, is the input for the temperature controller. Immediately downstream from the heaters, K-type Inconel TCs were installed to measure the temperature of the fluid (labeled Fuel TC and Oxidant TC in Figure 2). These are the same TCs mentioned briefly in 3.1.2. Insulation added around the coiled tubing to prevents heat loss to the environment as well as protect the aluminum framing and polycarbonate from melting. Additional insulation and a 120 V tape heater paired with a Watlow Precision Panel Mount Temperature Controller are used to maintain the temperature of the inlet tubing and upper section of the reactor.

3.2 Safety and Design 1 Amendments

For safety, an enclosure made of 1/4” thick polycarbonate built around the reactor that serves as a safety shield in case of a leak or failure. The reactor and its enclosure are located inside a fume hood to allow for ventilation of the reagent, fumes from the waste container, and any possible leaks. The frame was made from aluminum, 25 series 80/20 Inc. framing. Insulation around much of the reactor protects the polycarbonate and aluminum from the extreme temperature of the reactor.

During operation, switching from preheating to combustion requires switching from H_2O to fuel, which was accomplished by stopping and restarting the pumps and resulted in unreliable operation. This issue was

mitigated through the addition of directional flow valves upstream of the oxidant and fuel pumps, which allowed switching from water to fuel or oxidant without stopping the pumps. These valves allow the switching from the fuel and oxidant to water during cooldown, preventing backflow. On/off ball valves were placed inline, directly downstream of the pumps to allow for the priming of the pumps if necessary. For example, pump flow stops when air bubbles within pumps create a vapor lock. To fix this, the pump needs to be primed, which requires the opening of priming valves, and without inline valves, it would depressurize the system. Rapid depressurization during reactor operation would result in a rapid phase change, affecting flow rates, heat transfer properties, compressibility, temperature, etc., as well as causing potential damage to the pumps, closing the ball valve before priming prevented depressurization allows for safer and smoother operation.

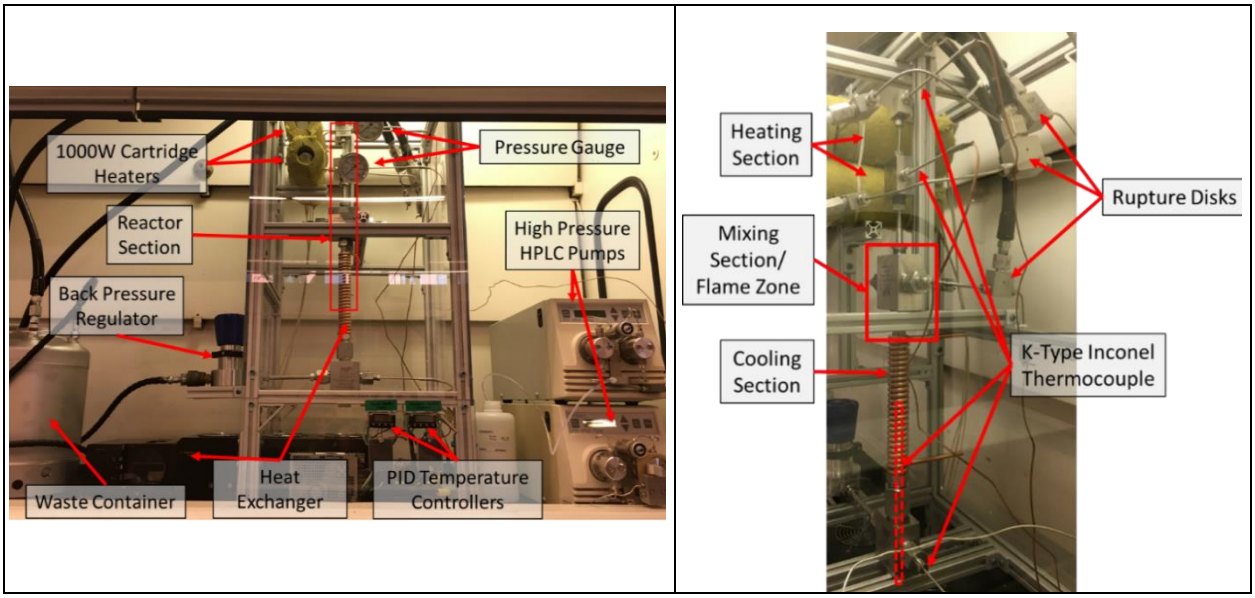

Figure 3: Inverted hydrothermal flame reactor assembly. Not pictured for clarity: Heating tape, insulation from the heaters through the reactor section.

3.3 Experimental Parameters

The goal was to validate that autoignition would occur in the reactor. Initial experiments used a premixed 30 mol% solution of EtOH in DI water reacting with reagent grade H_2O_2 (30 wt%). H_2O_2 was chosen for the initial oxidant because it was in a liquid state, controllable by readily available HPLC pumps. Ethanol was chosen as the fuel because of its low autoignition temperature and solubility in room temperature water. Dodecane was also considered; however, its insolubility in water was problematic for controlled dilution.

Due to the flow rate limitations of the pumps, as the oxidant was the restricting factor, the oxidant pump flow rate was set to a max of 10 mL/min ($Q_{(H2O+H2O2)}$). Maximum flow rates were found to reduce fluid heat loss in the system between the heater and the nozzle. The combustion of ethanol with hydrogen peroxide can be expressed with the following equation where ϕ_{AF} is the air-fuel equivalence ratio:

Eq. (1) $$[0.3C_2H_5OH + 0.7H_2O] + 9.78\phi_{AF}[0.184H_2O_2 + 0.816H_2O] \rightarrow 0.6CO_2 + 11.38H_2O$$

Table 1: Effects of φ_{AF} of flow rates

ϕ_{AF}	Q 30%mol Premixed EtOH (mL/min)	$Q_{(H2O + H2O2)}$ (mL/min)
1	1.63	10
2	0.82	10

3.4 Procedure and Results

The reactor was initially tested for autoignition. Autoignition is the occurrence of ignition with no external spark due to an increase in temperature. As noted in section 3.1.3, a larger flow rate pump was ordered for increased sheath flow because the flame temperatures were expected to be higher than originally anticipated so additional cooling would be necessary for extended operation. While awaiting this pump, testing for autoignition with no sustained flame was thought to be safe with the operation of a sheath flow at 10 mL/min.

The system was slowly preheated with to just above 400 °C using the flowrates in Table 1, for air-fuel equivalence ratio ϕ_{AF} =2 as well as operating the heat exchanger and sheath flow at 10mL/min. TC data was collected using PICOLOG 6. Initially, it was attempted to run at ϕ_{AF} = 2, however, the reactor did not have adequate insulation and heating to maintain a fuel temperature of 400°C at reasonable heater temperatures (<550°C) due to the low flow rates. The simple solution during the operation was to increase the velocity of the fluid through the system to avoid heat loss by running at ϕ_{AF} = 1. As noted prior, the oxidant pump running at 10mL/min was operating at its maximum flow rates, so it could not be increased further. Once 400°C was achieved in both the oxidant and fuel lines, the oxidant line was switched to H_2O_2. After running the oxidant for approximately 1 minute, fuel was allowed into the system by switching the fuel valve from H_2O to EtOH-H_2O mixture for 5 seconds, and then back to water. Only a small amount of fuel was allowed into the reactor for the autoignition test. In the experiment, ignition occurred rapidly, seemingly

without delay. Figure 4 shows that after a slight delay for the fuel to move from the pump to the reactor section, there was an immediate, a large spike in temperature recorded over a 14-second interval. As anticipated, following autoignition, a steady flame was not observed, likely due to the small-time interval over which the fuel was introduced. In contrast, during flameless oxidation, only a slight increase in temperature was observed. This gradual increase in temperature was not observed. Ideally, the reactor section thermocouple downstream of the co-flow nozzle would record the significant temperature increase upon autoignition. This thermocouple measured a maximum temperature of 815°C; however, upon further analysis, the thermocouple failed, melted, and was coated in molten titanium because the temperature downstream of the nozzle far exceeded the TC rated temperature. The nozzle and titanium liner additionally suffered severe melting, as shown in Figure 5. This suggests that the flame temp was well above the melting point of titanium (1668°C).

While the flow rates for an air-fuel ratio = 1 were used, H_2O_2 was introduced continuously for approximately 90 seconds before the 5 seconds of premixed 30%mol EtOH. After observing the ignition event, we believe that a small supercritical region was present at the nozzle outlet, though the Reactor Section TC, 4" downstream of the nozzle, was still reporting subcritical temperatures.

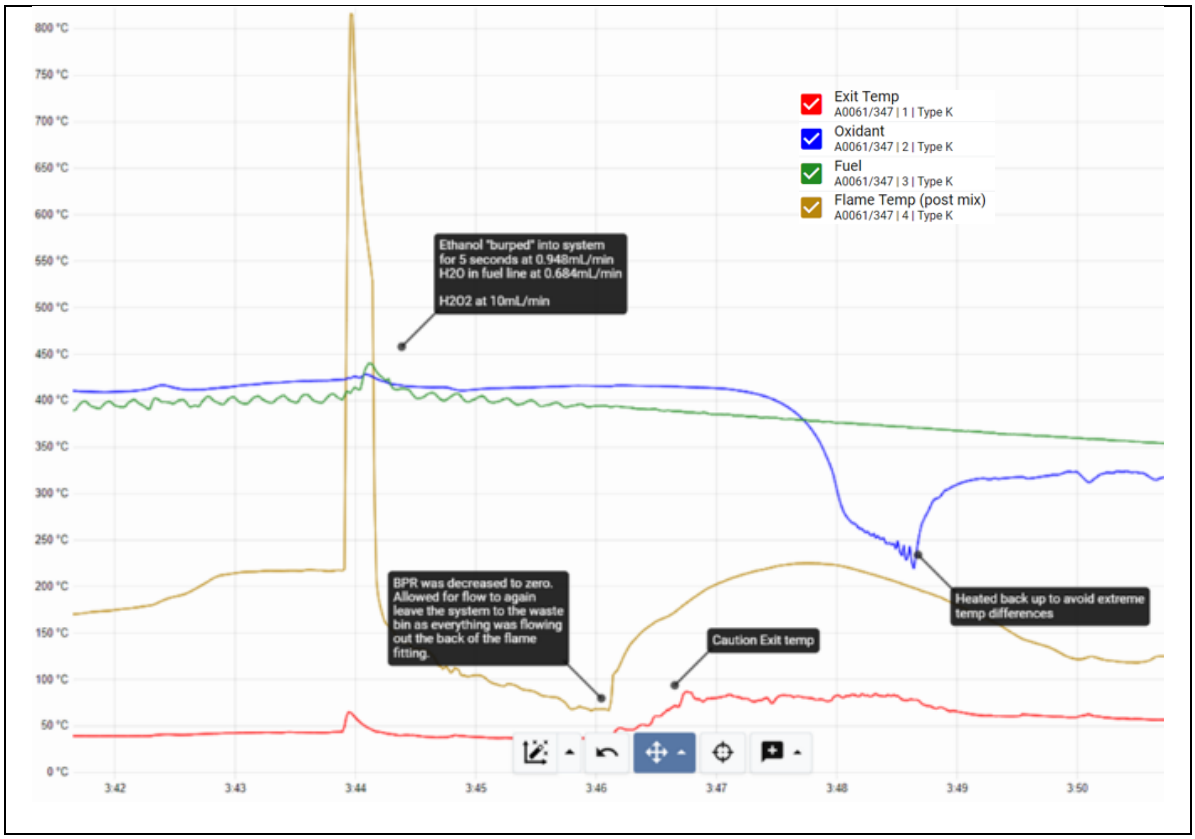

Figure 4: Thermocouple data from autoignition experiment: fuel EtOH30% in water, oxidant 30% H2O2 in water. The x-axis is representing time in hours: minutes. The spike in Reactor Section TC denotes the time and presence of a flame.

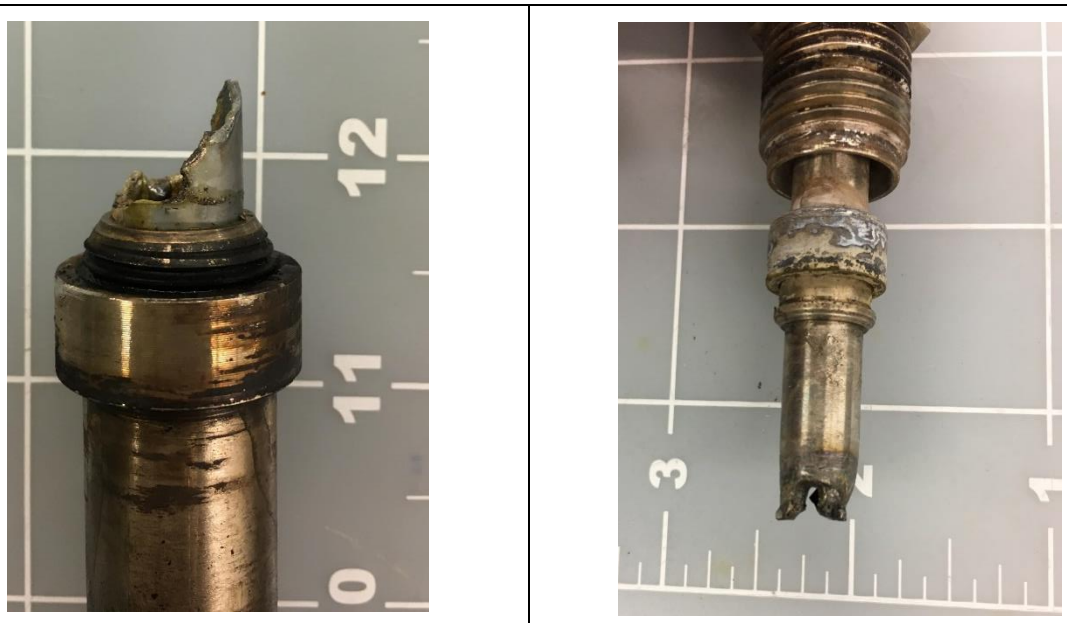

Figure 5: Left: Titanium liner melted during operation. Right: Oxidizer nozzle. Note that only the surrounding oxidant line melted while the center fuel line saw only minor discoloration.

3.5 Observations & Lessons Learned

3.5.1 Inadequate Sheath Flow Cooling

The presence of a liquid sheath flow in co-flow around the flame would create a stratified region with a supercritical region in the upper section of the reactors. Low sheath flow rates (10 mL/min) are not sufficient to provide enough cooling within the system. An analysis of Figure 5 led to the conclusion that a uniform sheath flow was not present. The two less melted edges of the nozzle were directly in contact with the sheath, whereas the melted edges were not. This non-uniform melting could be due to an insufficient flow rate resulting in a rapid increase in water temperature decreasing the cooling capacity of the sheath flow as it passed over the nozzle rather than the presence of a nonuniform sheath flow; or a combination of both.

Further, it was hypothesized that the melted nozzle and titanium liner could have been a result of flow stratification due to buoyancy effects. The liquid water has a much higher density than coupled with low flow rates may have resulted in a separation and concentration for combustible mixture near the nozzle rather than downstream.

Finally, due to low inlet velocities out of the nozzle and high-temperature gradient, it was possible that the flame “sticks” to the nozzle, i.e., when flame propagation speeds (FPS) are faster than the flow velocity, the flame will propagate upstream towards the nozzle. Therefore, the high FPS to flow velocity ratios is not desirable [33]. Flame speed, flow velocities, buoyancy, and position of the phase boundaries must all be considered to maintain a stable SCWO region in the inverted gravity configuration. Similar behavior was also observed in the inverted gravity flame reactors. The low nozzle velocities and buoyancy effects lead to the formation of the recirculation region [54, 55]. The reduction in the fuel heating value dilution with inert gas leads to longer flames and lower temperatures [56-59]. Some lessons from jet-stirred reactors could also be incorporated. The decreasing the fuel-air ratio results in displacing the flame downstream from the nozzle, which increases the reactor homogeneity and temperature reduction. However, reducing the fuel-air ratio below the flammability limit can result in the flame blowout [60-65].

3.5.2 Nozzle to Reactor Diameter Ratio

To avoid local wall heating, the nozzle to reactor diameter ratio could be increased.

i. A larger reactor cavity was explored to reduce the heating of the reactor walls and to prevent the titanium liner from melting. A greater distance between the nozzle and the reactor wall will provide a larger buffer region for cooling of reaction to the reactor wall.

ii. Nozzle design and knowledge of mixing times are essential. To prevent the nozzle from melting, faster velocities may be needed to delay the reaction to farther downstream and increase the separation between the jet nozzle and flame. The pumps were already operating at max flow rates during the failure of the reactor, so further increases to the nozzle required the purchase of new pumps or a decrease in the nozzle cross-sectional area. Reducing the diameters was a more desirable option of the two as a smaller jet would likely lead to a thinner flame, further increasing the flame wall to reactor wall distance. An increase in velocity would also reduce heat loss seen at lower flow rates.

iii. CFD simulations are needed to visualize the flow patterns in the reactor and verify these assumptions and the best options. An accurate CFD model is challenging to achieve because multiphase modeling of transport and mixing properties (I.e., density, specific heat (C_P), thermal

conductivity, surface tension, and viscosity) across the critical region is difficult to account for. Future experiments will aim to assist in validating a CFD model of the reactor.

3.5.3 Fuel Dilution

Prior autoignition research indicated that SCWO autoignition temperature varied from that of standard autoignition temperature and was dependent on fuel concentration [29]. Steeper's results also suggested that the autoignition temperature under SCWO conditions is different than those reported for air-fuel combustion (referred to as standard autoignition). Results showed that for methanol, with a standard autoignition temperature of 470 °C, under SCWO conditions and at concentrations of at least 6 mol%, autoignition occurred at 450 °C. This autoignition temperature could be further reduced to 390 °C for concentrations above 30 mol% [29]. Additionally, local, flameless, oxidation could occur at temperatures lower than the SCWO autoignition temperature; as the exothermic reaction increased local temperatures, delayed autoignition can happen [32]. Serikawa cautioned running with delayed autoignition as a buildup of fuel could result in a small, unexpected explosion [32]. Following the results from Steeper in which autoignition at SCWO conditions would occur at temperatures below that of at standard conditions (concentration-dependent), a premixed 30 mol% EtOH solution in H_2O was used to ensure spontaneous autoignition at 400 °C [29]. (Standard autoignition of EtOH is ~365 °C). In our initial experiments, methanol ignited spontaneously without delay (as evident by the sharp increase in temperature in the Reactor Section TC in Figure 4).

Cui et al. [66] compared the work by Augustine et al. [67] with that of Steeper [29], and found inconsistent results. Augustine found that the spontaneous autoignition temperature varied from 500-550 °C and was independent of fuel concentration [67]. It was deduced that autoignition temperatures are reactor dependent [66]. In hindsight, slowly increasing the fuel dilution of the premixed fuel from lower concentrations to find autoignition temperatures and the right operating conditions would have been a better method. Perhaps, running at 30 mol% EtOH solution is possible within this reactor configuration.

3.5.4 Back Pressure Regulator Failure

During the autoignition event, the Tescom back pressure regulator failed. The BPR could not hold pressure. This could have been caused by a rapid increase in exit flow temperature (BPR is only rated to 70°C), a

rapid increase in pressure at ignition (rated to 4000psi), or a seal leak due to large particulates (molted titanium chunks found in the reactor). Upon disassembly of the BPR, char and other particulates were observed within. The BPR was reassembled after these areas containing particulates were cleaned, and it was found to be in working condition again. A filter to prevent particulate build-up in the reactor is recommended for future designs.

4. DESIGN 2

4.1 Design 2.1 – Upright Hydrothermal Flame Reactor

Due to time and funding constraints, the redesign of the reactor was limited. It was decided that using parts from Design 1, a similar but more robust reactor would be built, and a more systematic approach would be taken to testing. CFD was deemed essential to assist in understanding the reaction and fluid dynamics in the system. The model was expected to be complex and take some time to build. Design 2 was designed to be tested in both an upright and inverted configuration and provide validation results to the model as required. It was first tested in an upright configuration to alleviate any concerns and unknowns due to buoyancy effects, specifically the possibility of fuel and oxidant trapping near the nozzle, which may have occurred in design 1. Hicks [33] had reported on the properties of an upright hydrothermal flame reactor with the use of a co-flow ethanol jet, and Serikawa had reported the results utilizing an inverted co-flow IPA jet with room temperature fuel [32]. These were to be used as a comparison to further the understanding of the system. Design 2 featured a longer and larger diameter reactor section to prevent the melting of the titanium liner. Additionally, in an attempt to avoid potential backflow out of the nozzle and/or to prevent the flame from sticking the nozzle, in the inverted gravity orientation, the diameters of the fuel and oxidant tubing were reduced to increase inlet velocity.

The following section outlines the modifications made to the reactor. If not explicitly noted here, parameters are the same as Design 1. The overall system schematic changed very little and is depicted in Figure 6.

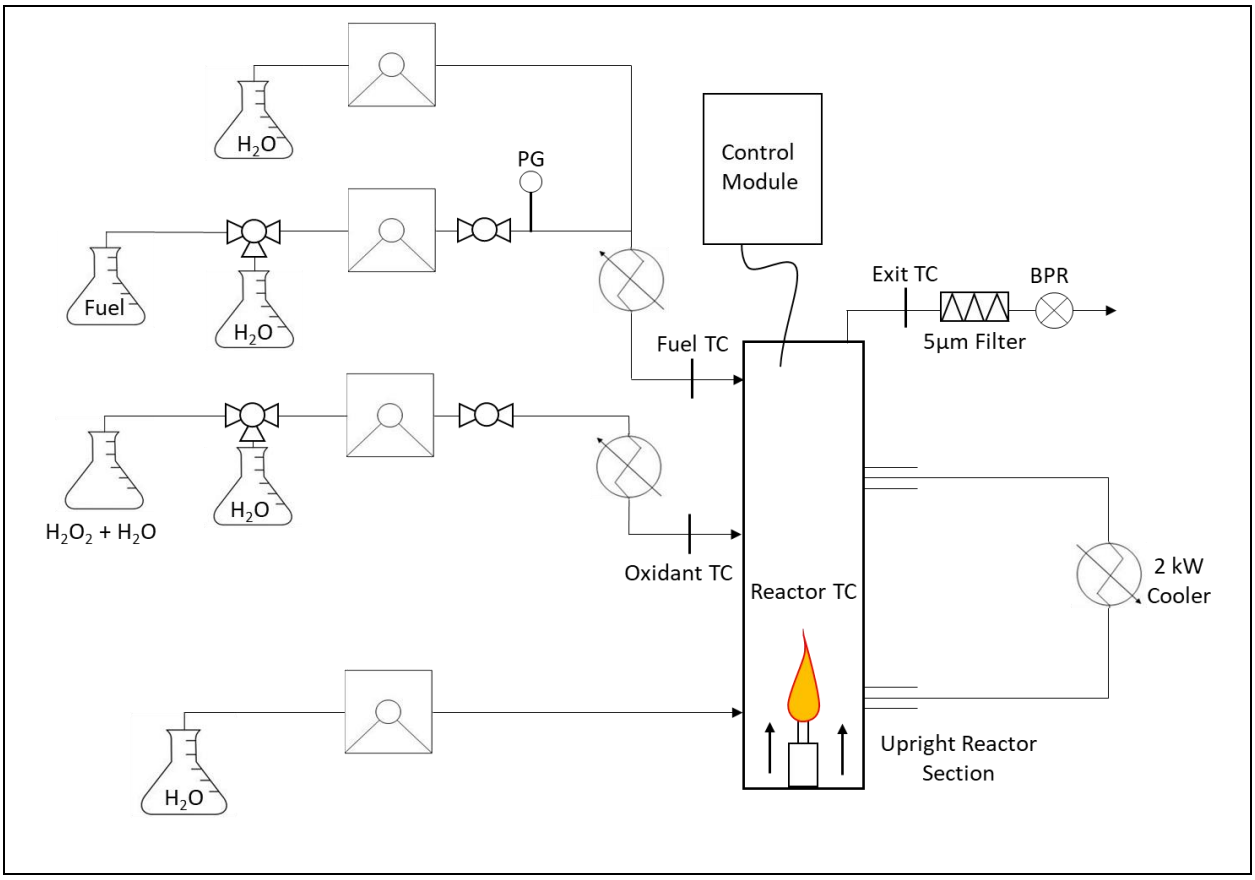

Figure 6: Schematic of Design 2.1, an upright hydrothermal flame reactor.

4.1.1 Reactor Section

The Inconel 625 cross fitting was drilled out to remove Titanium residue from the Design 1 meltdown and an adapter was added to accommodate the new, larger reactor section. Two custom Inconel 625 adapters converted the old 9/16" OD tube fitting to a 1.5" OD tube fitting and was located between "Custom Fittings 3 & 4" mentioned in Figure 2 and the reactor section. A 14" long, 1.5" OD (1" ID) 316SS tube lined with a pressure fit 0.997" OD (.955" ID) Titanium sleeve makes up the new reactor section. Figure 7 shows the new internal reactor diagram configuration, the change in reactor diameter, and adapters. The diameter of the fuel and oxidant lines were reduced to 1/16" OD (0.0225" ID) and ¼" OD (0.152" ID) IN625 tubing, respectively. As seen in previous reactors [32, 33], the nozzle was also slightly reconfigured with the fuel line extending approximately 1/16" from the oxidant tubing shown in Figure 7.

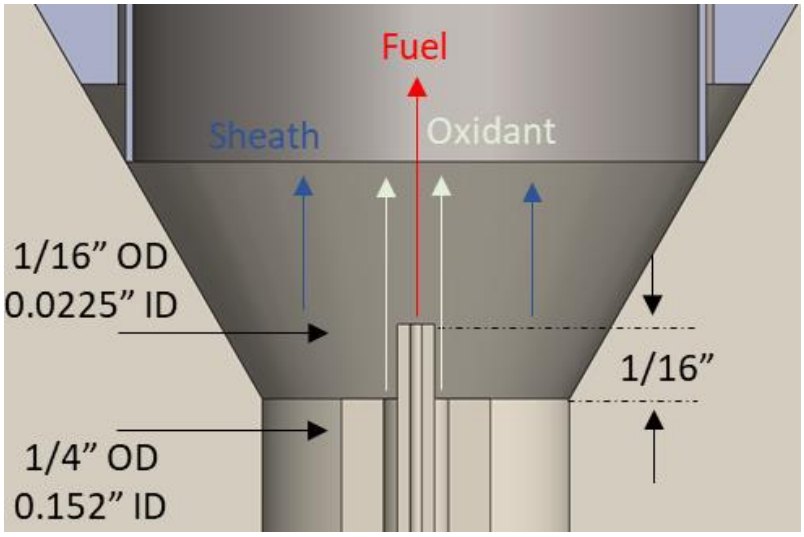


Figure 7: Nozzle configuration. Left: 3D model of nozzle located within the Inconel 625 adapter shown further in Figure 8. Middle: Nozzle close up showing Inconel 625 strips fuse-welded to the outer oxidant tubing to allow for disassembly if needed. Right: Nozzle centered within Inconel 625 adapter as modeled in the image to the left.

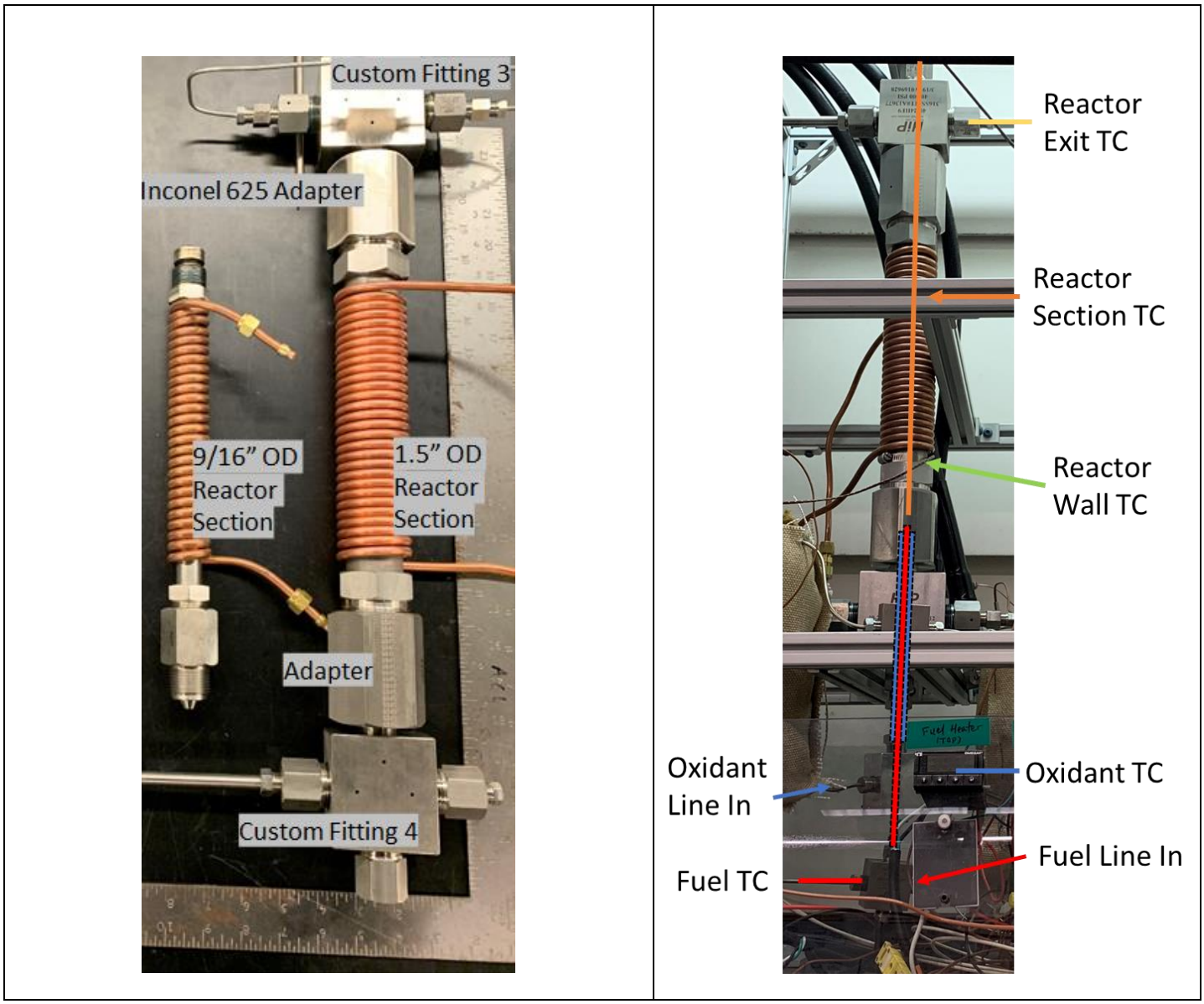

Figure 8: Left: Change in reactor section size from Design 1 (left) to Design 2.1 (right). Custom Fittings 3 & 4 are the same from Design 1 (refer to Figure 3). Right: Design 2.1 TC locations during operation. Shown without isulation or heating tape for better visual aid. Reactor appears slanted due to camera angle.

4.1.2 Insulation

A 1/8" thick thermally stable composite paper insulation sheet (R= 0.6) rated to 600°C was wrapped once around a layer of 1/4" thick ceramic fiber insulation sheet (R = 0.4) rated to 1175°C. These were added immediately between the cartridge heaters in the fuel and oxidant lines to just before the copper tubing

coiled around the reactor wall acting as heat exchanger on the reactor section. The purpose of this insulation was to maintain the temperature at low flow rates downstream of the heater, which reduces strain on the heaters and the materials. The heat exchanger was not used in the experiments thus far.

4.1.3 Back Pressure Regulator

To address the prior issues with BPR failure, a 5-micron in-line Swagelok filter was inserted just before the BPR to prevent particulates such as char from passing through.

4.2 Upright Reactor Analysis

The primary goals of the initial operation were to assist in CFD validation. Multiple temperature measurements are desired. Previously, the Reactor Section TC was located 4” away from the nozzle. By changing out the TC to a TC set to a different length, other internal temperatures could be obtained, but at only 1 measurement location per operation. During initial testing with the Reactor Section TC 1/8” and from the nozzle, as shown in Figure 8. In the upright configuration, it was challenging to achieve supercritical temperatures.

To assist in CFD verification, the reactor was first operated without sheath flow. The reactor section heat exchanger was OFF. The post reactor heat exchanger was left on as the system still required cooling as not to damage the BPR (<70°C Exit temperature). Temperature measurements from this configuration (shown in Figure 9) were far too low for ignition. To increase temperature, it was tested without sheath flow; the reactor section heat exchanger was off, the walls were insulated as described in section 4.1.2. To avoid overheating the BPR, an air heat exchanger was utilized by coiling 25’ of 1/8” 316SS tubing and exposing it to ambient air. From the results presented in Figure 9, it was determined that upright configuration could not be used auto-ignition, as the bulk fluid could not be raised to above supercritical temperature.

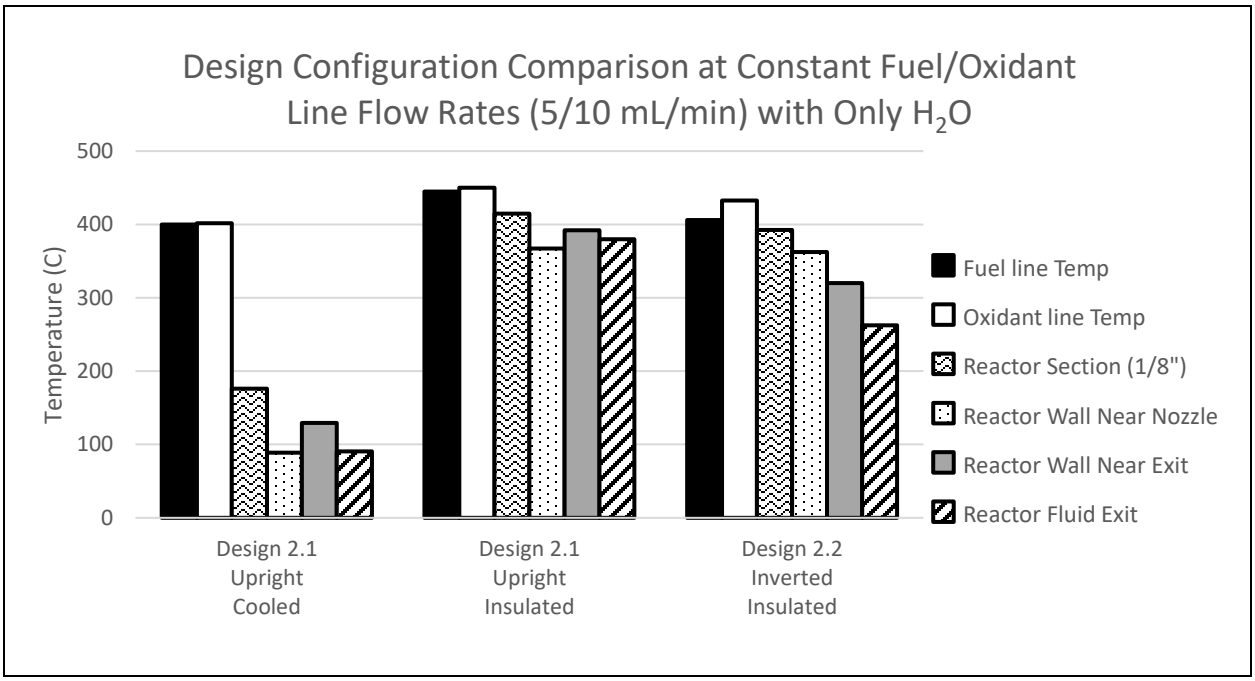

Figure 9: Comparison of reactor temperature due to design and configuration with H_2O flow through the fuel/oxidant line with flow rates of 5/10 mL/min, respectively.

Creating a supercritical region in the reactor within a reasonable start-up time required turning off the cooling heat exchanger and instead of wrapping the reactor section with insulation. The temperature set point of the cartridge heaters required to maintain oxidant and fuel temperatures were also found to be hotter than when operating in the inverted gravity configuration. The relatively high preheat conditions, as well as the high wall and fluid temperatures at both ends of the reactor, were concerning. To avoid plugging and re-dissolve potential salts in the reactor, a transition to sub-critical temperatures before exiting is required and was also challenging for this upright configuration. The temperature profile of the reactor was thought to be driven by buoyancy effects. The “cold” end of the reactor is 14”+ downstream and above the nozzle. During heating, it is possible that the SCW out of the nozzle rose and cooled as it progressed towards the reactor exit. As the water cools, it becomes denser and is likely to recirculate downwards before flushing out. Because of the density difference and possible bubbling effect, there was no consistent sc-region near the nozzle. For the Reactor Section TC to measure sc-temperatures at 1/8” from the nozzle, the entire reactor section needed to be at sc-temperatures, see Figure 9 (where sc-temperatures were observed at the 1/8” Reactor Section TC). Heating the entire reactor to supercritical temperature was not

desired because this would not provide a transition to subcritical for the desired solubility of salts and due to long warm up time.

4.3 Design 2.2 – Inverted Supercritical Water Oxidation Reactor

After the operation of the reactor in an upright configuration, the design was updated for an inverted configuration. The main motivation was to mitigate thermal stresses on the reactor and improving the start-up time. The modifications to the reactor are outlined below.

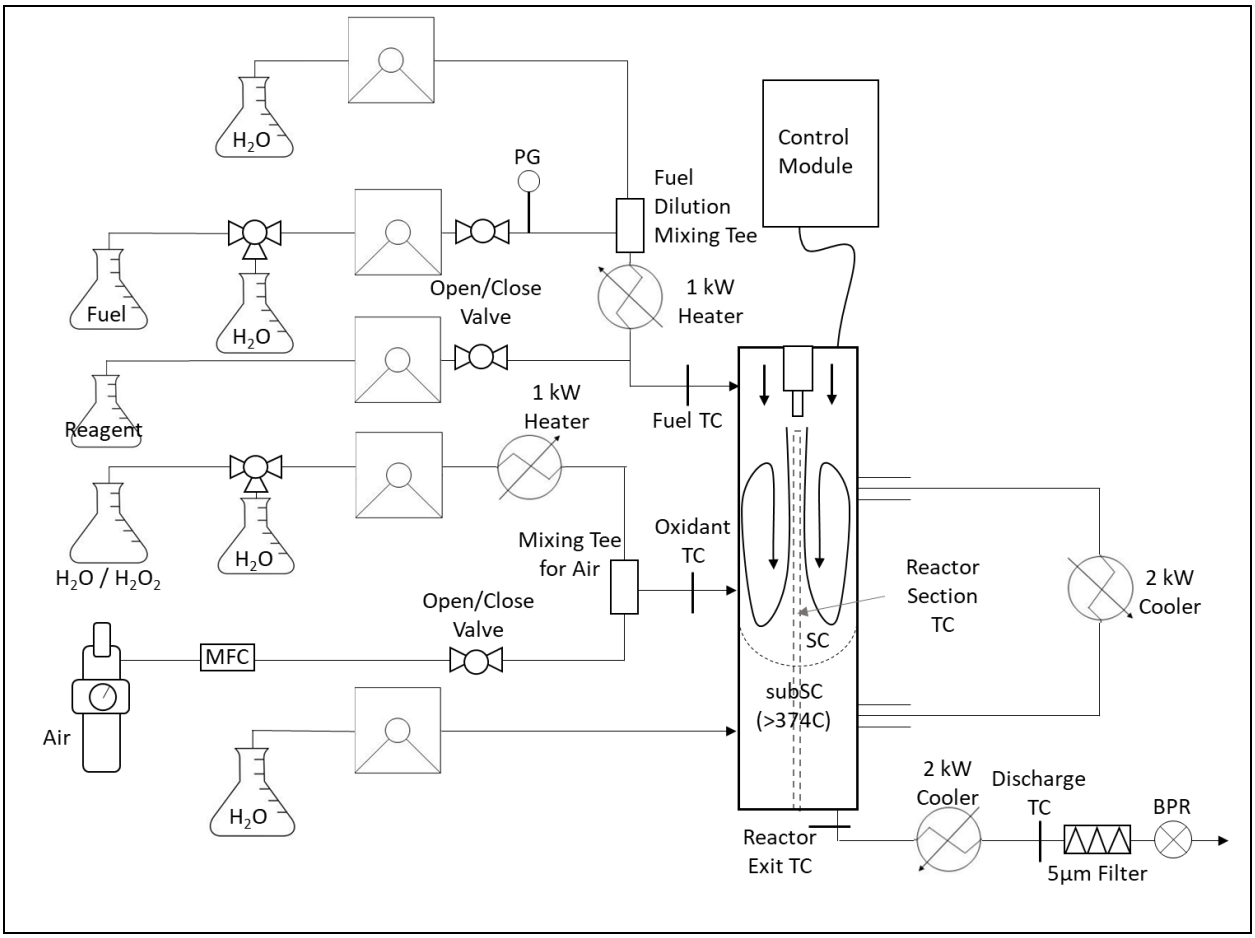

Figure 10: Reactor schematic of Design 2.2, Inverted SCWO reactor compatible with operation of air.

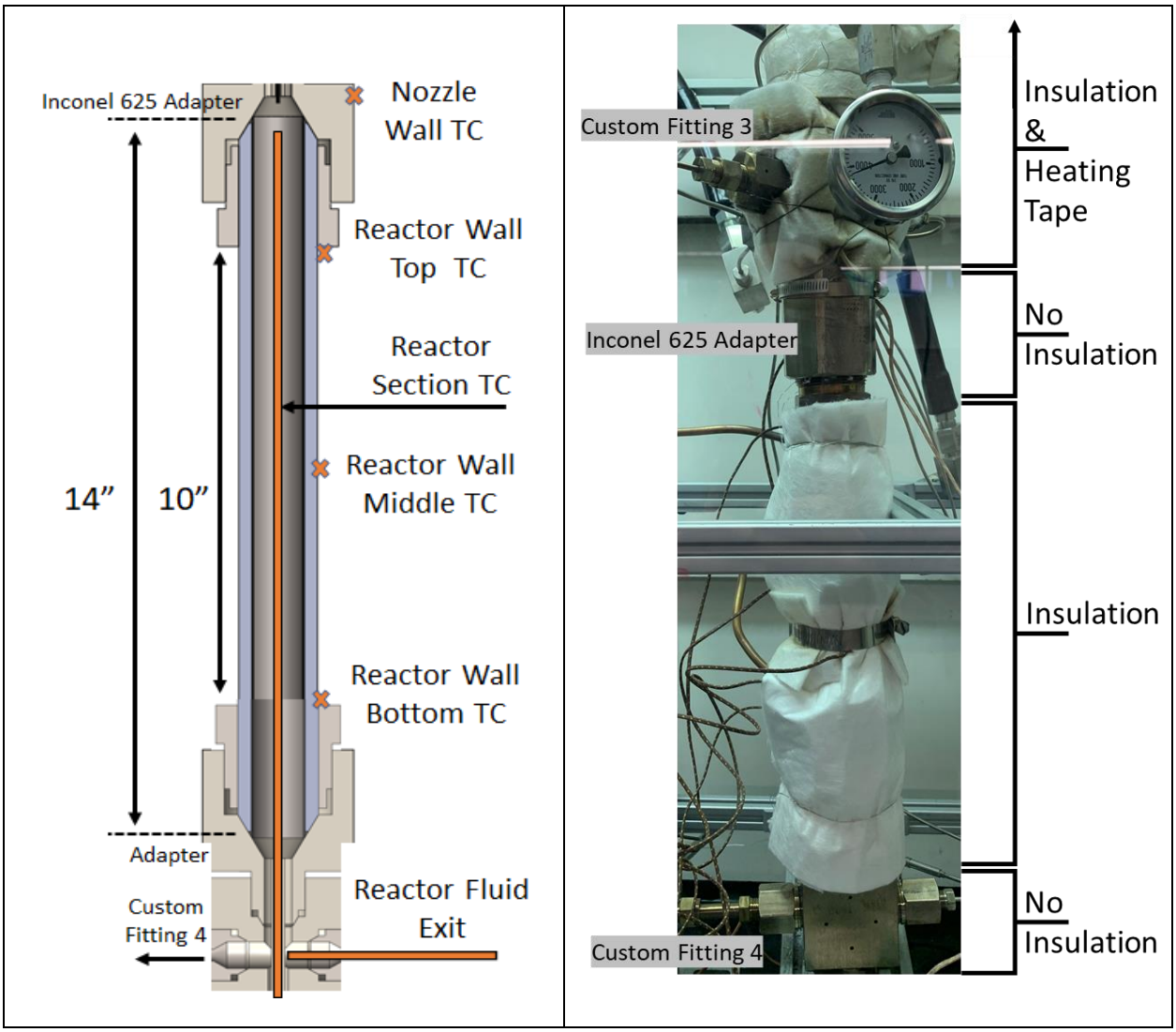

Figure 11: Reactor Section – Left: 3D model of Design 2.2 reactor section demonstrating TC locations. Not in the picture is Fuel and Oxidant TC located above the nozzle. Right: ISCWO showing the location of Insulation. Both: Custom Fittings 3 & 4 are the same as those outlined in Design 1 and Design 2.1.

4.3.1 Air and Oxidant Lines

An additional line was added to the existing oxidant flow path, allowing the reactor to operate with supercritical wet air as well as H_2O_2. A 6000 psi air tank and a SmartTrak 100 Sierra mass flow controller (MFC), along with an open/ close ball valve, control airflow into the reactor via a 1/8” 316 SS tube. The MFC can be operated manually or with a programmable module provided with the product. While using air, the oxidant pump that previously controlled the flow of H_2O_2 introduces water to be mixed with the air. As mentioned earlier, the air has very low solubility in subcritical water at STP, but it is fully miscible in SCW.

The added water maintains a high concentration of water in the reactor. Most importantly, water is used to heat the oxidizer stream to provide sufficient temperature for ignition and the operation. The SCW and air are mixed within an Inconel tee (labeled “Mixing Tee for Air” in Figure 10) to form sc-wet air. When running water or H_2O_2, closing the valve upstream of the tee on the airline prevented the backflow.

4.3.2 Reagent Line

A 1/8” Inconel 625 HiP cross replaced the original tee (Custom Fitting 1 from Figure 2), allowing for an additional inlet into the fuel line. The additional inlet was connected to a 515 HPLC Waters pump via a 1/8” 316SS tube and was used for the addition of a reagent into the system, as necessary. Although beyond the scope of this thesis, it is anticipated this valve will be used with future work to test for the complete destruction of DMMP as a reagent. Referencing Figure 10, the reagent line can be introduced to the fuel line after the heating section. This is important because some reagents, such as DMMP, begin to break down at temperatures lower than the critical point of water (374°C). The DMMP decomposition produces methylphosphonic acid (MPA) as a refractory intermediate species [68]. As DMMP and MPA are corrosive and not in SCW, it is desirable to avoid reaching sc-temperatures or starting DMMP decomposition within the nozzle as it would form insoluble phosphates that would potentially lead to plugging of the reagent line. Thus, the injection below the critical point (374°C) is preferred when operating with DMMP. It is estimated that the reactor was operated at ~550°C for ~14.4 seconds would facilitate the complete destruction of MPA [68]. Prior reactors, such as Serkiawas inverted transpiring wall reactor, have shown the feasibility of operating with a room temperature fuel inlet [32]. In the Serkiawas reactor, the reactor section was heated externally to internal fluid temperatures of 470°C, varying from Design 2.2 in which the reactor section was no actively heated but maintained sc-temperatures as a result of the preheated fuel and oxidant lines. This heated reactor section likely assisted in driving the reaction, providing the energy that would otherwise be present if the fuel were preheated. Considering the differences in reactors, it is predicted that if the fuel line is preheated to achieve autoignition and sufficient recirculation exists, the fuel line may be cooled to <200°C and still sustain operation due to the exothermal heat from the reaction.

4.3.3 Back Pressure Regulator and Additional Heat Exchanger

As discussed in 4.2, operating Design 2.1 at supercritical temperatures required the use of a heat exchanger to reduce the temperature of the liquid before BPR. During initial oxidation experiments in Design 2.2, the Tescom BPR failed twice. Upon fixing the BPR, the Kalrez O-Ring was found to be compromised. Failure was detected to have been a result of inadequate cooling. During operation, the exit temperature reached temperatures higher than 50°C wherein, CO_2 would be supercritical at 25 MPa (Critical point: 7.4 MPa, 31°C). While the BPR is rated to higher temperatures, $scCO_2$ is known to be an aggressive solvent. An additional 2kW ALX-2000-P400 Koolance cooling system along with a Sentry TSR Sample Cooler was added between the 5-micron Swagelok filter and the reactor section to provide additional cooling before the BPR. With this additional heat exchanger, the exit was held at <25°C, and no failures have occurred.

4.3.4 Pumps

Extended operation of the Waters 515 pumps running with 30 wt% H_2O_2 caused pump failure, likely due to hydrodynamic cavitation and damage to seals or O-rings. The Waters 515 HPLC pumps were exchanged for Teledyne SSI MX-series pumps capable of 10mL/min at 5000 psig and Teledyne SSI HF-series pump, capable of 300mL/min at 10,000 psig. All pumps can be remotely controlled from a laptop via an RJ45 connection necessary for automation of the reactor discussed further in 4.3.6.

4.3.5 Insulation and TCs

The insulation mentioned in 4.1.2, was updated; additional insulation was placed immediately downstream the cartridge heaters in the fuel and oxidant lines to just before the reactor section and again, over the copper coiled heat exchanger to the bottom of the reactor section, see Figure 11. The fitting at the top of the reactor section was left uninsulated because the threaded gland was made from 316 SS and the fitting from Inconel 625 and due to the differences in the thermal conductivity and coefficient of thermal expansion between the 316 SS gland and the Inconel 625 fitting a leak would occasionally occur. When left unheated, this junction had less frequent leaks. This part of the reactor can be eventually be welded. Another TC to measure wall temperature near the top of the reactor was added, see Figure 11.

4.3.6 Solenoids and Controls

For testing of CWA destruction, the remote operation will be required. An ongoing design goal for remote control is working to both simplify and render the reactor safe during operation with CWA. To accommodate this requirement, the manual directional flow valves located upstream of the pumps outlined in 3.2 were replaced with computer programed solenoid valves. These solenoids are controlled by the same computer that controls the pumps (mentioned in 4.3.4). The control module gathers TC data, controls the heaters, and controls the MFC. Note that near-complete remote operation is possible from this computer. The only non-controllable aspect of the reactor currently is the BPR and sample collection; however, the BPR can be set to a specific pressure. Future work aims to fully automate the operation.

5. RESULTS

5.1 Operation with H2O2

The operation of the SCWO Reactor with the use of H_2O_2 and ethanol as oxidants and fuel are presented here. The results present a range of 2-7mol% dilution of ethanol in H_2O and 30%wt reagent grade H_2O_2.

Data collected in this chapter utilized a version of the reactor described in Chapter 4.2. No sheath flow was introduced during the operation. The reactor section was insulated as described in 4.2.5 and the heat exchanger was always off. All fuel concentrations reported were premixed in water. The reaction of ethanol and hydrogen peroxide shown in Eq. (2):

Eq. (2) $$[C_2H_5OH] + \omega\phi_{AF}[30wt\%H_2O_2] \rightarrow \mathrm{A}\ CO_2 + B\ H_2O$$

Eq. (3) $$[C_2H_5OH] + \omega\phi_{AF}[0.184H_2O_2 + 0.816H_2O] \rightarrow \mathrm{A}\ CO_2 + B\ H_2O$$

For stoichiometric, with $\phi_{AF} = 1$

Solving Eq. (3) yields $\omega = 6$ and operation with excess air can be rewritten as:

Eq. (4) $$[C_2H_5OH] + 6\phi_{AF}[0.184H_2O_2 + 0.816H_2O] \rightarrow 2CO_2 + 9H_2O + \mathrm{Excess}\ O_2$$

Additionally, H_2O_2 is known to decompose during heating within the reactor [69]:

Eq. (5) $$1\ H_2O_2 \rightarrow 1/2\ O_2 + 1\ H_2O$$

5.1.1 Preignition Operation

5.1.1.1 Preheat

Preheating the system usually takes around 2 hours, the system reaches equilibrium faster with higher flow rates. System response is sensitive to flow rates, and low flow rates (<5mL/min) cause fluctuations in temperature readings due to high heat loss and underdamped PID settings. Conversely, high flow rates (>10mL/min) creates inadequate heat transfer from the cartridge heater. From the First Law:

Eq. (6) $$\mathrm{Q} = \dot{\mathrm{m}} C_P \Delta T$$

as the mass flow rate increases, so does the required rate of heat transfer, Q. As the heater was designed around a maximum flow rate of 10mL/min, at the higher flow rate reactor was difficult to heat. The optimal operating conditions are between 7-10 mL/min for TC stability. However, flow rates above and below can

still be accommodated by changing PID setting and/or increasing the temperature of the cartridge heaters though higher than used for steady-state operation. Typically, for flow rates of 10mL/min, fuel and oxidant line heaters were set to ~430°C to achieve a fluid temperature of 400°C.

5.1.1.2 Steady-State Operation with H_2O

SCW is injected into the reactor to study the flow profile, pseudo-phase change to obtain data for validating the CFD models. As the system approached equilibrium, the temperature field depends on the flow rates. After equilibrium, the TC data from +/- one minute were averaged, the maximum and minimum values associated with the variation were recorded. If the preheat temperatures varied more than 10 °C, the dataset was considered as a separate case. The maximum and minimum temperatures are represented by error bars. Some additional TC positions such as Reactor Wall Middle and Reactor Wall Nozzle (Figure 11) were added as requested for additional CFD validation. The 5/5, 5/10, 9.3/4.7, and 30/10 (fuel/oxidant flow rates in mL/min) cases were performed only once, no error bars are reported. The results are presented in Figure 12 and Figure 13.

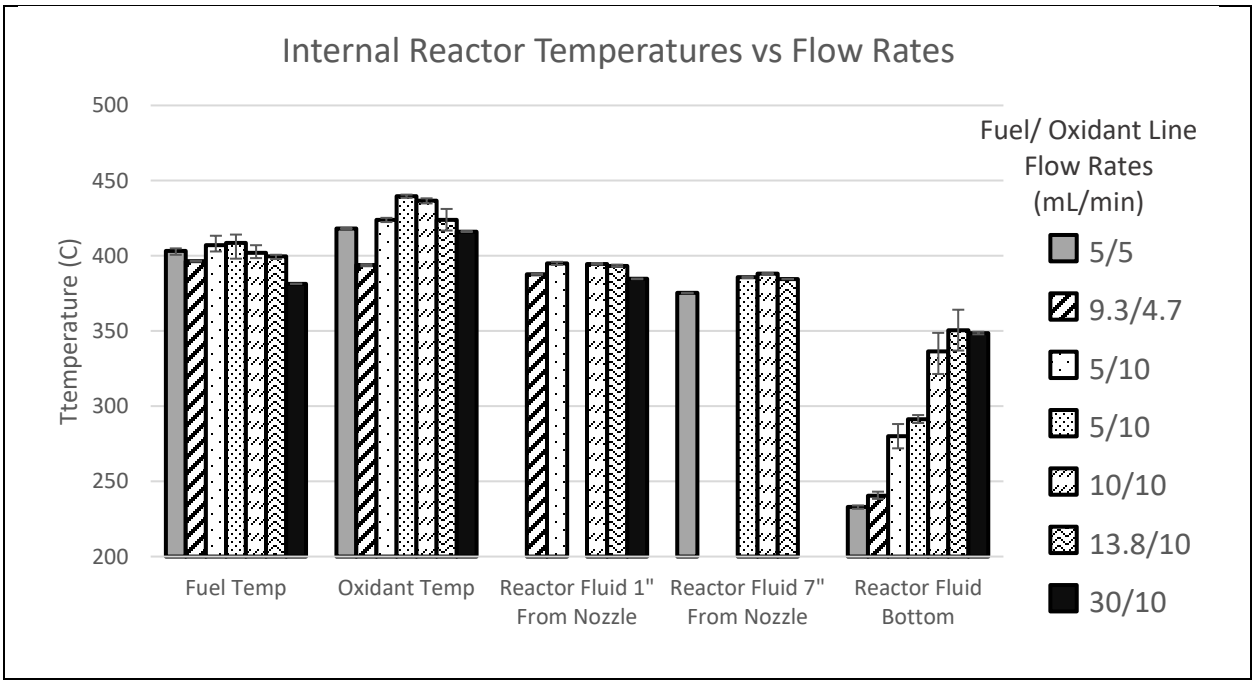

Figure 12: Reactor fluid temperatures in Design 2.2 during operation with only H_2O at varying flow rates. Missing data indicates no data recorded.

When running H_2O_2, the reactor typically operated at the maximum oxidant flow rate (10mL/min) due to the maximum 30% oxidant concentration. At fuel and oxidant line flow rates of 10 mL/min (10/10), running only DI H_2O, Figure 12 shows only a 6.4 °C difference between 1" to 7" distance from the nozzle. Between the reactor midpoint (7" TC) reading and the reactor fluid bottom reading, a large temperature decrease of 51.8 °C and transition to subcritical water was observed. This transition from supercritical to sub-critical water was observed for all flow rate cases and is likely the cause of the larger heat loss in the bottom half of the reactor.

As the pump flow rates vary, both mass flow rate and C_P affect heat loss. The pseudo-critical point of water, or temperature at which C_P is largest, occurs at 385°C for a constant pressure of 25 MPa. This spike in specific heat (seen in Figure 1) and phase change create a local, nearly isothermal region. At this point, significant heat transfer is required to reduce the temperature below 385°C. However, before and after, heat loss occurred more rapidly. Except for the 5/5 case (where the 7" Reactor Section TC measured 374°C leading to the assumption that the C_P jump occurred sooner), for every other case, the measurements 7" from the nozzle fall right around 385°C. Furthermore, for the cases in which data for 1" and 7" are present, a larger drop in temperature was observed from the preheat measurement to 1" location, where then the temperature remained relatively constant to 7", typically only varying from ~394 to 385°C. It would follow then that these fluids would transition to subcritical lower in the reactor section where they cool more rapidly.

Further, SCW is a compressible fluid, and the density across the critical point varies significantly, as shown in Figure 1. As the fluid temperature drops below the critical point, the volumetric flow rate and fluid velocity will slow due to an increase in density. The effects of flow rate and heat loss can be observed in Figure 12, where the Reactor Fluid Bottom temperature varied consistently with flow rate. Using these assumptions and the temperature profiles of each case, nominal residence times within the reactor were calculated and presented in Table 2. Apart from the 5/5 case, large leaps in residence times (>50s) seem to correlate with the trend in temperature at the reactor bottom mentioned. The longer the fluid remains in the reactor, the more heat loss occurred.

Table 2: Nominal residence times in reactor Design 2.2 for various flow rates and preheat temperature. Flow rates correspond to those presented in Figure 12.

Pump Flow Rates, H_2O (Fuel/Oxidant Line in mL/min)	Preheat (Fuel/Oxidant Line) (°C)	Nominal Residence Time (s)
5/5	403/418	422.5
9.3/4.7	395.6/393.8	266.1
5/10	407/424	186.4
5/10	409/440	196.9
10/10	402/437	133.9
13.8/10	400/424	138.5
30/10	381/416	104.9

The wall temperature readings shown in Figure 13 appear similar to the reactor internal temperature readings shown in Figure 12. These wall TC locations, depicted in Figure 11, are located out the outer surface of the reactor. There was less variance between the wall temperatures reported for each fuel concentration, and the wall temperatures follow the same trends as the internal fluid TCs. The noteworthy exception is the “Reactor Wall Nozzle” measurement. As mentioned in Section 4.2.5, and shown in Figure 11, the fitting on which the thermocouple was located was uninsulated and cooled to ambient conditions, which caused more convective heat and radiative loss compared to the other walls TCs, which were in thermally insulated locations.

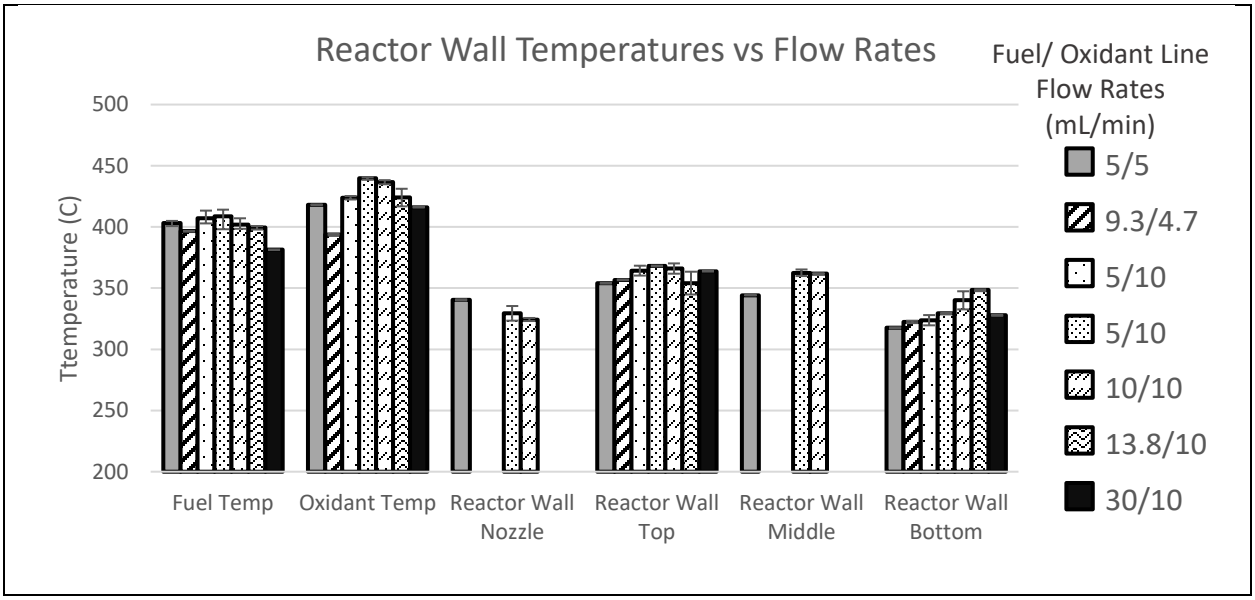

Figure 13: Design 2.2 reactor wall temperatures during operation with only H_2O. Missing data indicates no data recorded.

5.1.1.3 Cool Down

Cool down from fuel/ oxidant line operating temperatures takes more than 2 hours. On cool down, if the temperature of the liquid falls too low below that of the reactor walls, the reactor is likely to form leaks. Considering mismatch in coefficients of thermal expansion and in the thermal inertia of the fittings, these leaks are likely to occur when the inner walls are cooling faster than the external fittings. The relative shrinking/ expansion of the fittings becomes uneven and produces leaks which are much more prevalent in joints of mismatched materials, such as Inconel and 316SS.

5.1.2 Effects of Air Fuel Ratio

Table 3: Flow rates through fuel and oxidant pumps during operation at $\boldsymbol{\phi_{AF}}$ = 1.1 & 1.5 for varying EtOH concentrations in H_2O.

Fuel Concentration (%mol)	ϕ_{AF}	Fuel Pump Flow Rate Premixed Fuel (mL/min)	Oxidant Pump Flow Rate 30wt% H_2O_2 (mL/min)
3	1.1	9.4	10
	1.5	6.9	10
4	1.1	7.2	10
	1.5	5.3	10
5	1.1	5.9	10
	1.5	4.3	10
6	1.1	5	10
	1.5	3.7	10
7	1.1	4.4	10
	1.5	3.2	10

Air fuel ratios (ϕ_{AF}) of 1.1 and 1.5 were tested using pump flow rates presented in Table 3 to study the effect of excess air in the system and find optimal operating conditions. At higher fuel percentages, the effects of ϕ_{AF} were noteworthy. Other than the expected drop in temperature in both wall and reactor sections for higher ϕ_{AF}, significant fluctuations occurred in the reactor measured by the Reactor Section and Fluid Temperature Reactor Bottom TCs. Although not without some fluctuation, the Reactor Section TC data remains relatively constant at ϕ_{AF}=1.1. When switching to ϕ_{AF}=1.5, however, in addition to the fluctuations observed at ϕ_{AF}=1.1, Figure 14 shows a larger periodic oscillation in the reactor section TC that was also observed. This large oscillation seemed to follow the underdamped nature of the fuel line presented in Figure 14 but was more amplified; while the fuel behavior was the similar, these periodic

oscillations were either not present or less present at ϕ_{AF}=1.1. Further, the increase in oxygen in the reactor created a noticeable increase in temperature instability at the Fluid Temperature Reactor Bottom TC. At the bottom of the reactor for ϕ_{AF}=1.1 in the experiment presented in Figure 14, the average outlet temperature was 362°C. At this subcritical temperature, the oxygen would be less miscible and bubbling out of the fluid. From Figure 17, the reactor fluid bottom temperature was subcritical for all cases of fuel concentration except 2%. Additionally, large amounts of CO_2 were present as products from the combustion. The instability at the reactor fluid bottom TC was somewhat periodic, for both the small, infrequent fluctuations observed when ϕ_{AF}=1.1 and larger, more frequent fluctuations when ϕ_{AF}=1.5. Due to the specific miscibility of oxygen and CO_2 in water, at constant mass flow rates it was expected the gases would flush out of the system at regular rates. The rapid fluctuations are attributed to presence not miscible oxygen in the liquid water exiting the reactor, as the two-phase mixture bubbles through the exit; the thermocouple measurements are affected by the rapid change in the heat transfer properties of the effluent. Tests of ϕ_{AF} between 1.1- 1.5 and beyond were not conducted as fluctuations were expected to only increase from 1.1. In future operation, operation with H_2O_2 at ϕ_{AF}=1.1 is recommended.

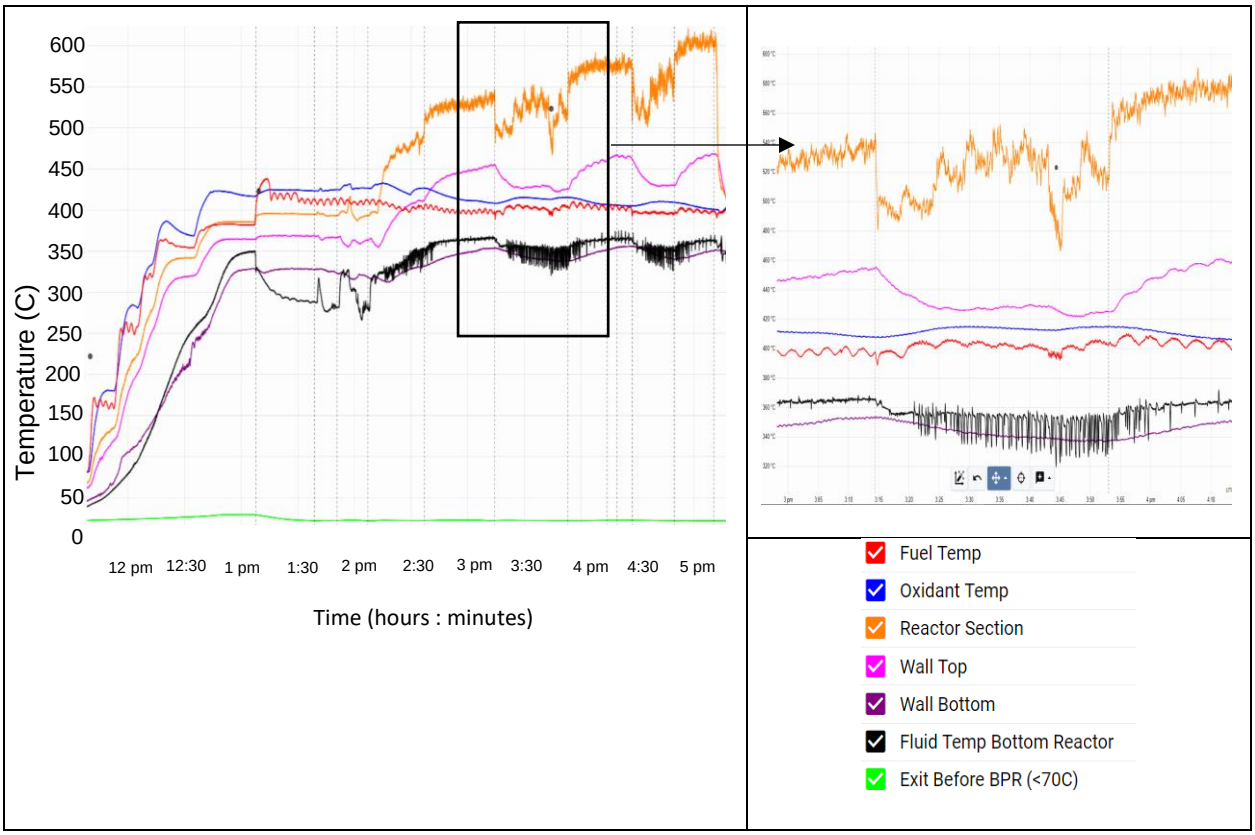

Figure 14: Typical operation of the reactor with H_2O_2 showing preheat and oxidation with 5, 6, & 7%mol EtOH at $\boldsymbol{\phi_{AF}}$= 1.1 & 1.5. Highlighted region shows the transition from $\boldsymbol{\phi_{AF}}$ =1.1 at 5% to $\boldsymbol{\phi_{AF}}$=1.5 at 6% and then to $\boldsymbol{\phi_{AF}}$=1.1 at 6%mol EtOH. Noteworthy is the change in Fluid Temp Bottom Reactor TC and oscillations of the Reactor Section TC. This reactor section TC is located 1" from the nozzle during this experiment.

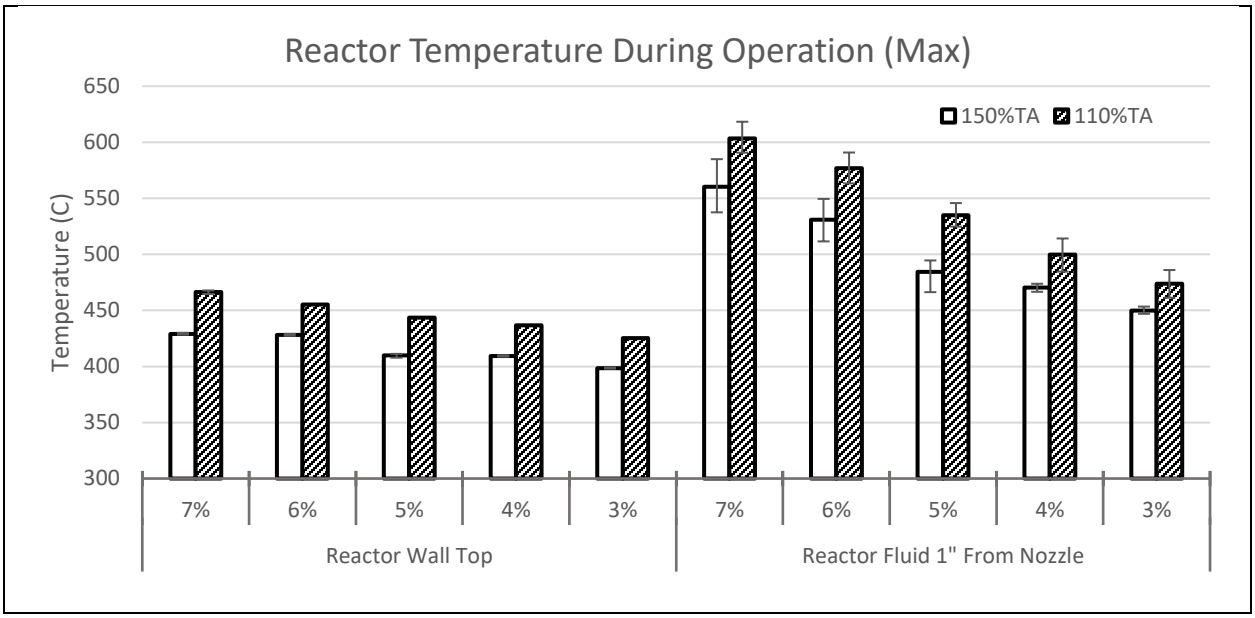

Figure 15: Temperature effects at 2 different TC locations due to change in $\boldsymbol{\phi_{AF}}$ at various fuel concentrations. 150% TA is equivalent to $\boldsymbol{\phi_{AF}}$=1.5 (and the same for 110%TA = $\boldsymbol{\phi_{AF}}$=1.1) where TA denotes the theoretical (stoichiometric) air conditions.

5.1.3 Effects of Fuel Dilution

The data showing the effect of fuel dilution by water during operation at ϕ_{AF} =1.1 are presented in Figure 17 andFigure 18. There were two main goals in running these experiments. First, to completely destroy DMMP, a reactor temperature of 550°C for a residence time of 14.4 seconds are required to destroy MPA [68, 70]. To meet these system requirements, achieving a reactor section temperature > 600°C and determining residence times associated was desired. Samples were taken to verify complete oxidation of EtOH during these experiments using Raman spectroscopy, see Figure 16. The second goal involved conducting multiple experiments with varying reactor section TC locations for each fuel concentration to validate CFD validation. As only one TC measuring reactor section temperature at a specified distance from the nozzle could be used at a time, the results presented represent multiple data sets compiled similarly to the data presented in 5.1.2.

The highest temperatures were observed at 7mol% EtOH in which the reactor section 1” from the nozzle measured 603.5°C. The calculation of residence time is complicated by the rapid density change and it should be estimated based on the CFD analysis; in particular, the actual time spent at temperatures needed

to fully decompose MPA is important. *Ex-situ* Raman analysis of effluent from the reactor during operation at $\phi_{AF} = 1.1$ was analyzed and no concentrations of ethanol above the detection limit were present (Figure 16b). Therefore, referring to Eq. (2) the ethanol was completely oxidized to CO2 and water.

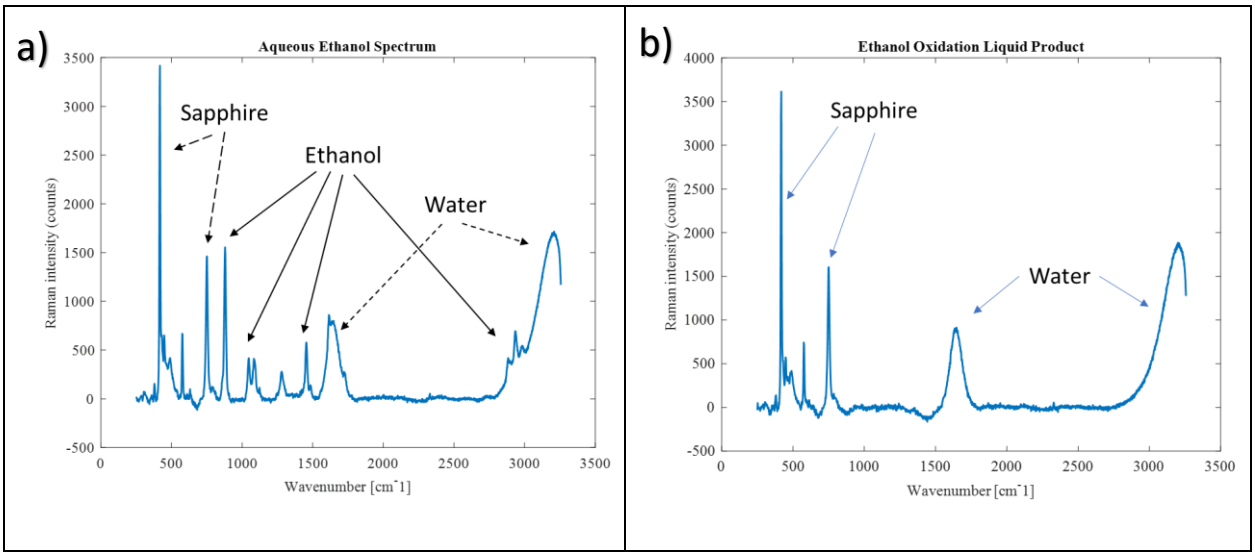

Figure 16: a) Raman spectra of typical aqueous ethanol mixture. b) Raman spectra of effluent from the operation at $\boldsymbol{\phi_{AF} = 1.1}$ with H_2O_2 and air showing complete oxidation to water and gaseous (CO_2).

The local temperature at 1" from the nozzle increased almost linearly with increasing fuel concentration, at a rate of approximately 31.9°C/ %mol. Conversely, the temperature at the bottom of the reactor slowly decreased in temperature from 384°C at 2% to 362°C at 7%. At the center of the reactor section, only a small increase in temperature (17°C) is observed from 2%-6% (data not reported at 7" for 7%). This is an indication of shifting flame position as a function of the heating value of the fuel stream. These results are presented in Figure 17.

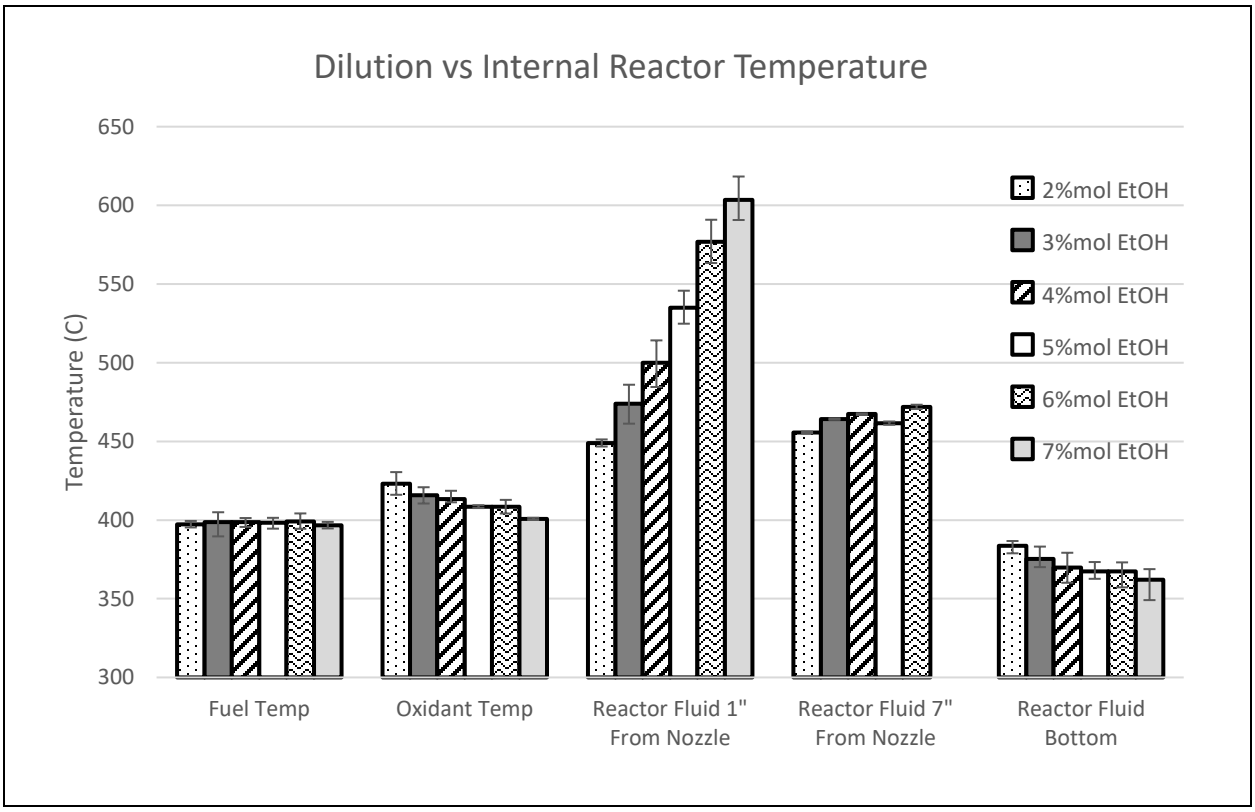

Figure 17: Reactor fluid temperatures during operation of the Design 2.2 SCWO reactor with $\boldsymbol{\phi_{AF} = 1.1}$ operating with H_2O_2 and varying concentrations of EtOH.

Surprisingly, as the concentration increased, the temperature at the reactor bottom decreased as the maximum temperatures observed in the reactor continued to increase 1" from the nozzle. Although 7%mol EtOH had a 1" reactor section TC measuring 154.6°C hotter than 2%mol EtOH, its temperature at the reactor bottom was 21.6°C cooler. It is hypothesized this trend was due to a lower mass flow rate associated with running higher fuel concentrations. As discussed in 5.1.1, higher heat loss is expected as mass flow rates are reduced. To further understand heat loss, nominal residence times within the reactor section were calculated and are given in Table 4. Because volumetric flow rates represent rates at the pump, these nominal residence times provide a more complete understanding of the time the fluid spends in the reactor as a result of volumetric flow rates and fluid temperatures. In section 5.1.1.2, operating only with water, the residence times had a larger variance. For comparison, operation with water for the 5/10 case is representative of the 6mol% EtOH case, while 13.8/10 is representative of the 2mol% EtOH case (refer to Table 2 &Table 4). A difference in residence time of >47.9 seconds was the primary factor for additional heat loss. During operation with fuel, the difference in nominal residence time from 2mol% to 6mol% EtOH

was reduced to 7.5 seconds. The significant reduction in residence time, therefore, does not solely explain the magnitude of the difference in heat loss within the reactor at higher fuel concentrations. The difference may be due to the location of the 'flame" in the reactor. At 2%mol fuel dilution, the highest temperature during operation is observed 7" from the nozzle, and it maintains a higher temperature at the bottom of the reactor than observed for any other fuel concentration. It is likely that for lower concentrations, this reaction zone moves downstream while the higher fuel concentrations occur in an upper region, closer to the nozzle. More Reactor Section TC data and CFD simulations would be needed to validate these hypothesized explanations.

Table 4: Estimates of flow parameters during the operation of the Design 2.2 Reactor.

Local Fuel Concentration (premixed)	Residence Time (s)	Flow Rate of Fuel Pump (mL/min)	Flow Rate of Oxidant Pump (mL/min)	V of Fuel at Nozzle (m/s)	Re of Fuel at Nozzle	V of Oxidant at Nozzle (m/s)	Re of Oxidant at Nozzle
2%mol	17.6	13.8	10	8.16	17449	0.17	2090.8
3%mol	21	9.4	10	5.52	11809	0.17	2090.8
4%mol	23.2	7.2	10	4.20	8986	0.17	2090.8
5%mol	25	5.9	10	3.41	7296	0.17	2090.8
6%mol	25.1	5.0	10	2.88	6168	0.17	2090.8
7% mol	25.3	4.4	10	2.51	5363	0.17	2090.8

During operation, the wall temperature changes followed the same pattern observed for internal fluid temperatures. At the top of the reactor, the temperatures rose with the onset of the SCWO reaction (Figure 18). At the bottom, the reactor wall bottom temperatures fell to resemble the trend in temperatures of the fluid at the bottom (Figure 17). Although the internal fluid temperatures rose ~31.9°C/%mol EtOH, wall temperatures only rose an average of 11.9°C/%mol EtOH. Recalling safe reactor wall operating temperatures briefly mentioned in 3.1.1, operation of the reactor walls were rated to 650°C and temperatures of the wall never rose above 468°C, indicating that future applications of the reactor can withstand the higher fuel percentages.

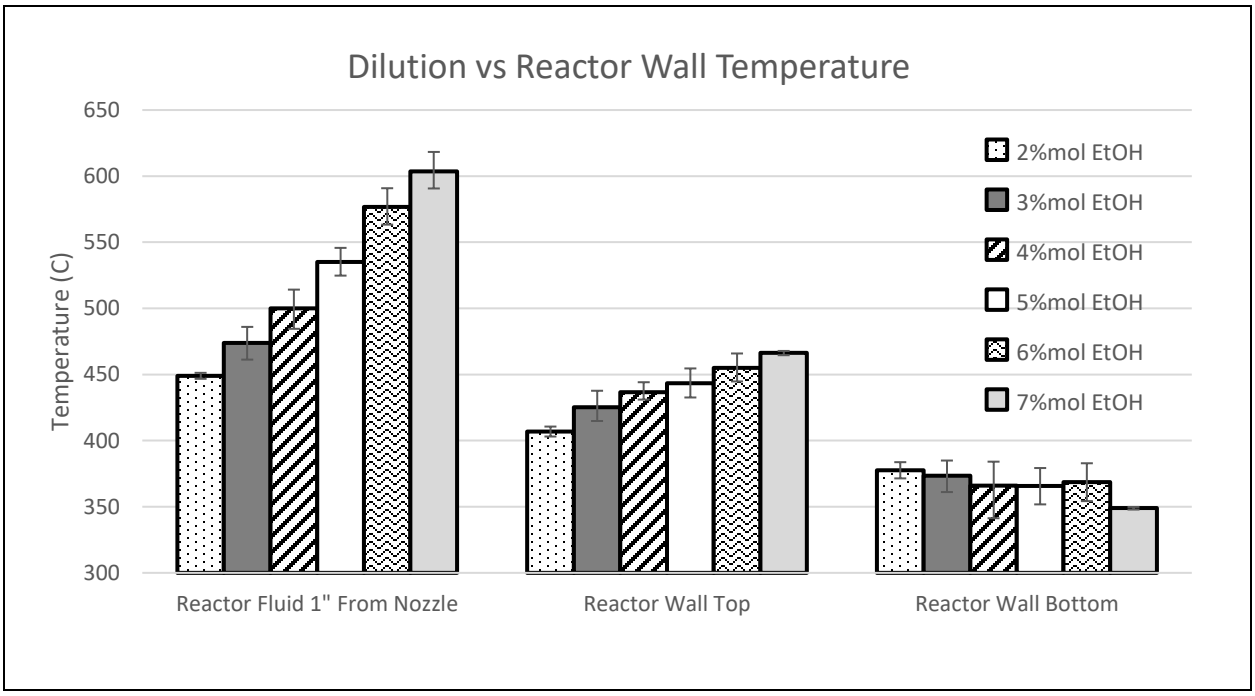

Figure 18: Reactor Design 2.2 wall temperatures during operation with H_2O_2 and varying concentrations of Ethanol at $\boldsymbol{\phi_{AF} = 1.1}$.

Two fuel ratios are important in understanding the dynamics of the system: the local fuel dilution and overall fuel dilution. The local fuel dilution is the molar ratio of the fuel and water in the fuel line. The overall fuel dilution is the molar ratio of all inputs into the reactor section, which incorporates additional water from the oxidant line that further dilutes the reaction. Local dilutions tested varied from 2-7%mol EtOH and corresponded with overall fuel dilutions (before reaction) from 1.20-2.17%mol (see Table 5). While the overall fuel dilutions varied only slightly, there was 1.77x less water and the same amount of fuel (/kg basis) in the 7%mol case than at 2%mol. This reduction in water flow rate reduced the amount of excess water (or diluent) for the reaction to heat and the flow rate of the fuel nozzle observed in Table 4.

Table 5: Comparison of local vs. overall molar fuel % in the reactor.

Local Fuel Dilution (Premixed Fuel)		**Overall Fuel Dilution in Reactor Before Combustion**		
%mol EtOH	%mol H_2O	%mol EtOH	%mol H_2O	%mol O_2
2	98	1.2	95.4	3.35
3	97	1.53	94.26	4.21
4	96	1.76	93.4	4.83
5	95	1.93	92.78	5.29
6	94	2.06	92.29	5.66
7	93	2.17	91.89	5.95

5.1.4 Pump Troubles

The introduction of 30%wt H_2O_2 by the HPLC pumps proved to be troublesome. The instability of 30%wt H_2O_2 at room temperature, dissociating to O_2 and H_2O as shown in Eq. (5), seems to cause cavitation, leading to failure of the pumps. Four Waters 515 HPLC pumps were used throughout the experiments; the pumps had to be fixed often. Others have reported having parts on hand to fix the pumps as failure occurs; however, this is costly, and ultimately not practical for operation [69]. The use of H_2O_2 as an oxidant is not recommended if an alternative is available.

5.2 Operation with Air

The data for operation with air are limited, as the testing is still on-going. Switching to air was desirable to reduce the operational costs and improve reactor reliability. Additionally, the cost (not including the destruction of the pumps) of oxidant when operating the reactor with H_2O_2 was approximately $25/hour. Switching to operation with air reduced this cost to $5/hour. The analysis includes the price of bottled air.

The configuration for operation with air varied slightly from that of H_2O_2 (as outlined in Section 4.3.1). The main difference was the mixing of room temperature dry air with SCW to form sc-wet air. The effect of this within the reactor when running only H_2O is presented in Figure 19. As expected, the mixture cooled during mixing but remained at supercritical temperatures if the initial preheat was sufficient.

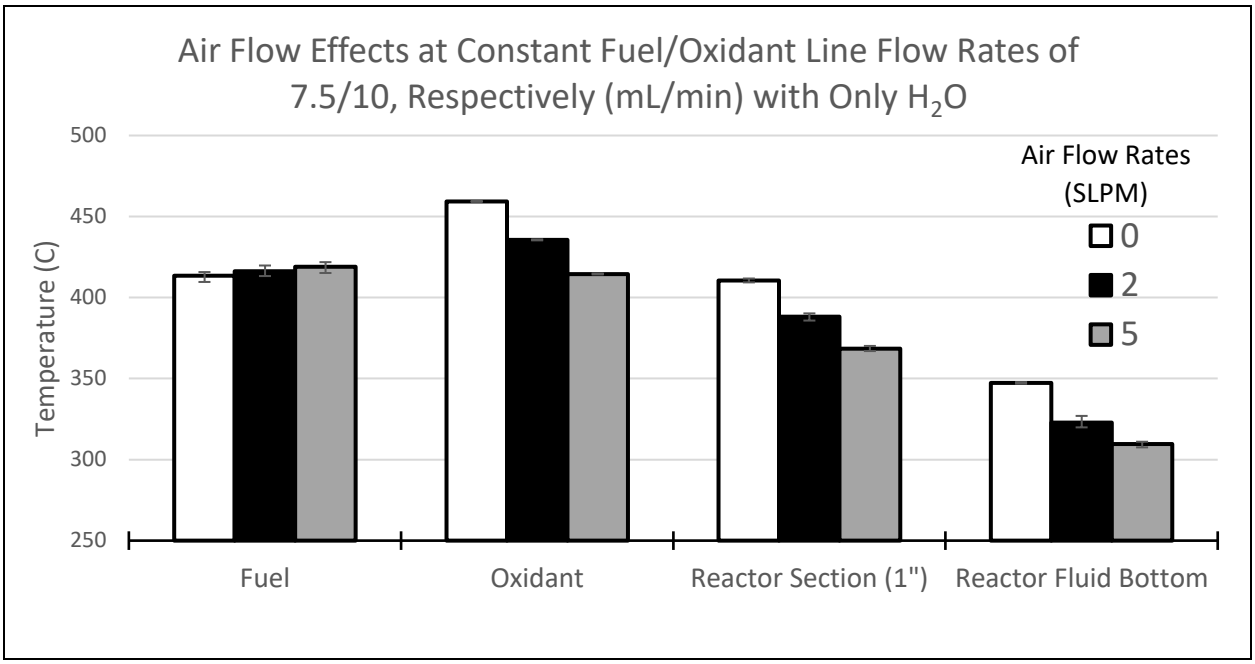

Figure 19: Effect of mixing room temperature, dry air in the oxidant line with preheated SCW to form sc-wet air before Oxidant TC at various air flow rates.

Combustion of ethanol with sc-wet air is described by the following simplified equation:

Eq. (7) $$[C_2H_5OH] + \omega\phi_{AF}[O_2 + 3.76N_2] \rightarrow 2CO_2 + H_2O + 3.76\omega\phi_{AF}N_2$$

$$\omega = 3$$

Table 6: Flow Rates and Stoichiometric Air : Fuel Ratio Used During Experiments with Air

Premixed Fuel Concentration (mol %)	ϕ_{AF}	Fuel Line Flow Rate (mL/min)	SC-Wet-Air Flow Rates	
			Water Flow Rates (mL/min)	Air Flow Rates (SLPM)
4	0.6	7.4	10	2.89
	1.2	7.4	10	5.79
	1.8	7.4	10	8.76

The stoichiometric ratio of EtOH to O_2 is represented by ω. Flow rates presented in Table 6 for air were computed using conservation of mass and are reported in standard liters per minute (SLPM – 0°C, 101 kPa); these units are used as input for the MFC control. Figure 20 shows the results of fuel and SCW-air mixture. Only the flow rate of air was varied during operation as shown in Table 6. The highest reactor temperature (i.e., of 473°C at 1" from the nozzle) was observed when operating fuel-rich with $\phi_{AF} = 0.6$. This was unexpected as the highest temperature should occur close to $\phi_{AF} = 1$. The observed results can

be explained by preheat temperatures. As shown in Figure 19, sc-wet air temperatures decreased as the flow rate of air increased. Comparing the increase in Flame and the inlet temperatures rather than maximum temperature shows that the maximum increase of 67°C occurred at $\phi_{AF} = 1.2$. Other conditions yeilded 62°C for $\phi_{AF} = 1.8$, and 57°C for $\phi_{AF} = 0.6$. Additionally, as shown in 5.1.3 (H_2O_2 experiment), the increase in airflow may have caused the reaction to occur downstream of the 1" reactor section TC. Further experiments and/ or CFD are needed to gain a better insight.

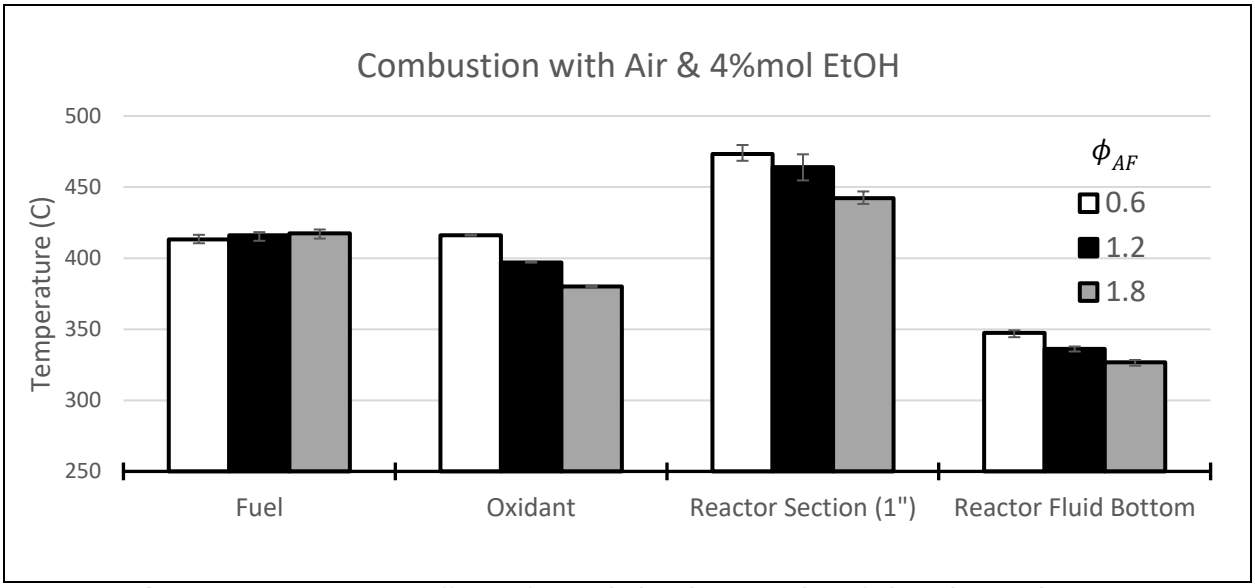

Figure 20: Temperature effects of AFR during the operation of air and 4%mol EtOH.

We will compare operation with air vs. H_2O_2. First, the reactor operation at 4%mol EtOH shows a reactor section TC (1") is lower by 36°C when operating with air (see Figure 21). For the two cases compared in Table 7. Air case had a slightly higher ϕ_{AF} than H_2O_2 (1.2 vs 1.1, respectively). On the other hand, the air case had a 0.2 mL/min higher flow rate of 4%mol EtOH into the system. Neither of these small variations in the experiments likely caused the difference in temperatures at the Reactor Section TC. More likely, this change is due to the overall composition makeup. Air cases have added nitrogen in the system through the overall fuel to oxygen ratio is similar to H_2O_2 cases that have only water as diluent. Additional diluent requires more energy to reach the same temperatures. Because of added nitrogen, the overall molar concentration of fuel is lower in the air cases. During operation with H_2O_2, a 0.3%mol decrease in overall molar fuel ratio resulted in approximately a 30°C drop in temperature. Provided in Table 7 for comparison is the case H_2O_2 and 2%mol local fuel dilution that presents a more similar overall fuel dilution. Operation

of 2%mol local EtOH with H_2O_2 resulted in a 1" Reactor Section TC measurement of 450°C, a significantly closer temperature to that of air (difference of -14°C).

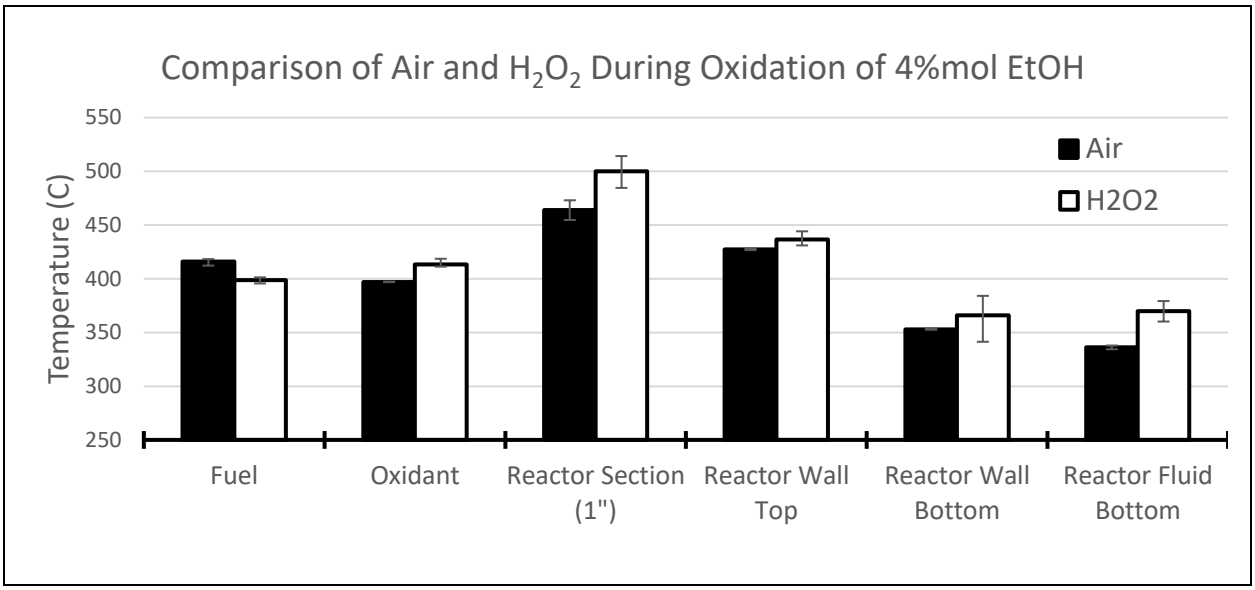

Figure 21: Comparison of air and H_2O_2 operation at 4%mol EtOH. Note that overall dilutions and $\boldsymbol{\phi_{AF}}$ are not the same and are further described in Table 7.

Table 7: Comparison in reactor section composition before oxidation between similar operations with air and H_2O_2. For residence times, after initial mass flow into the reactor was calculated, density was assumed to be that of water for simplicity. 2% case was provided for comparison of overall dilutions.

Operation with	**%mol Fuel**	ϕ_{AF}	**Fuel Flow Rate (mL/min)**	**Water Flow Rate (mL/min)**	**Oxidant Flow Rate**	**Overall Fuel Dilution in Reactor Before Combustion**			
						%mol EtOH	%mol H_2O	%mol O_2	%mol N_2
30wt% H_2O_2	4	1.1	7.2	0	10mL/min	1.76	93.40	4.83	0
air	4	1.2	7.4	10	5.76 SLPM	1.29	78.44	4.63	15.64
30wt% H_2O_2	2	1.1	13.8	0	10mL/min	1.2	95.4	3.35	0

Another observation is the lack of temperature fluctuations at the reactor exit. Based on operation with H_2O_2 (Figure 14), higher gaseous species concentration in the effluent should lead to greater fluctuations. Surprisingly, as shown in Figure 22**Error! Reference source not found.**, increasing the airflow rate from 2.5 to 5 SLPM decreased the fluctuations. During combustion with the production of CO_2, the reactor fluid

bottom fluctuation remained constant. This was hypothesized to be due to a large gaseous presence that shifted the effluent flow from liquid with bubbles to wet airflow.

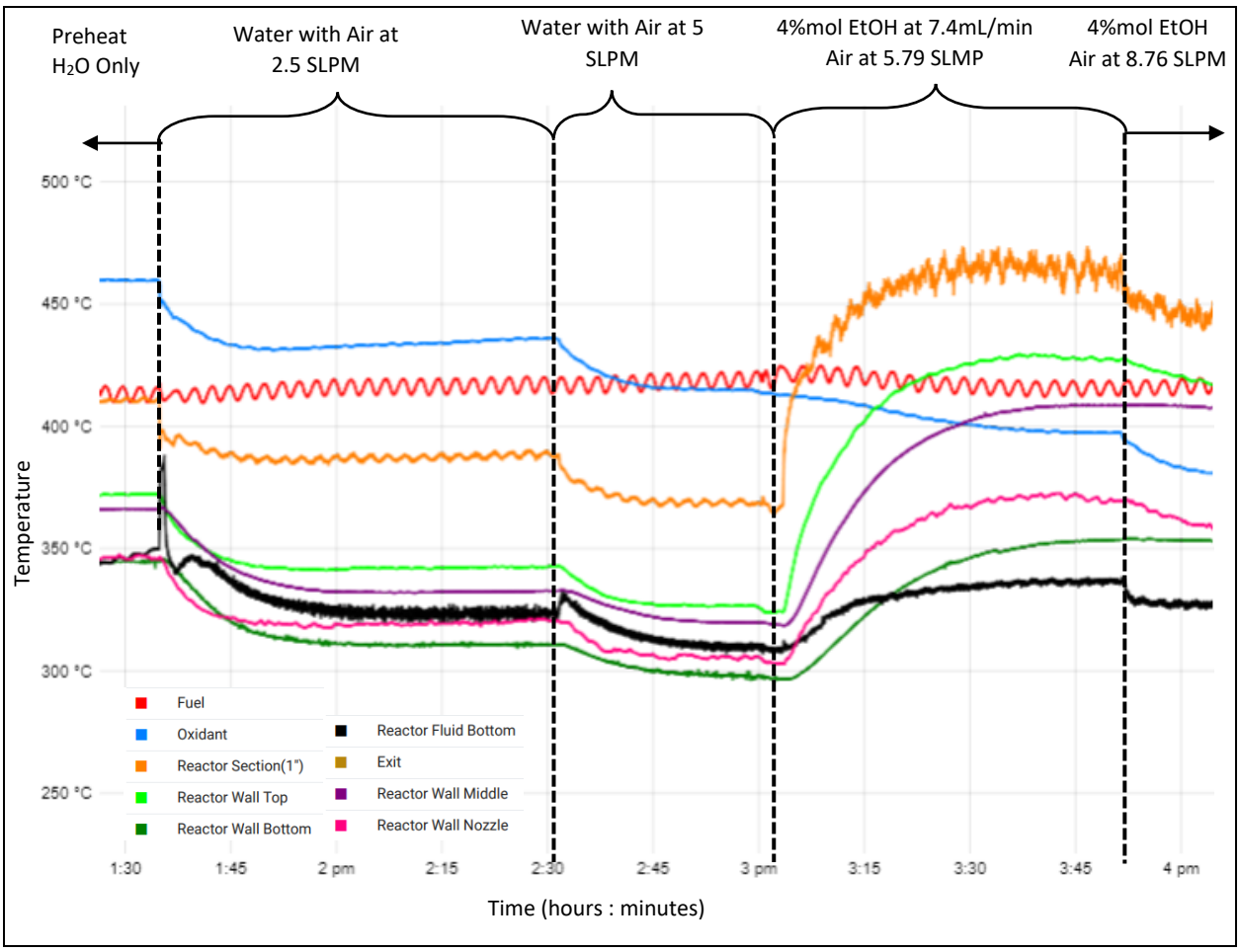

Figure 22: Segment of a typical run during combustion of air and EtOH. More exactly, operation with 4%mol as presented in Figures 19 & 20.

6. CONCLUSION

The most recent reactor (Design 2.2) was optimized over three iterations. Design 2.2 facilitates flameless oxidation in an inverted configuration. For safe operation, the design utilizes an improved nozzle design and 1" ID reactor chamber. The reactor was successfully operated with compressed air or hydrogen peroxide as the oxidant. Fully remote operation is possible except for setting the back-pressure regulator, which must be done manually before the reactor start-up. An additional heat exchanger and filter upstream of the backpressure regulator prevent reactor failure due to a loss of pressure during operation. In the event of plugging, high-pressure limiters on the pumps, as well as the rupture disks, prevent catastrophic failure of any fittings. Although not yet tested, active reactor wall cooling is possible with the use of a heat exchanger as well as an internal sheath flow of water. The final overall design is small enough to fit within a fume hood and is small enough to be considered portable.

The reactor operation was tested up to 600C, which exceeds the minimum temperatures required to decompose DMMP and MPA — 550°C with ~15 second residence time [68]. During testing with oxidant 30 wt% hydrogen peroxide in water and 7 mol% EtOH in water, the reactor section reached 603.4°C at ϕ_{AF} = 1.1 with an approximate residence time of 23.5 seconds. Examination of effluent with Raman spectroscopy showed complete destruction of EtOH. Relatively low reactor wall temperatures during operation of 7%mol EtOH suggested possible operation with higher premixed fuel concentrations. However, one must be careful to avoid the onset of flaming combustion. When operating with hydrogen peroxide, optimal oxidation conditions occurred at ϕ_{AF} = 1.1. Large fluctuations and instable reactor temperatures, likely due to an increased presence of gaseous bubbles in two-phase effluent at ϕ_{AF} = 1.5 were observed. Though it was convenient to use hydrogen peroxide as an oxidant, it was found to have a detrimental effect on the HPLC pumps, rendering them inoperable after approximately two days of operation. Pump repair was costly and required constant monitoring during the operation.

More recent tests of the reactor with air as the oxidant were conducted but have been limited (due to time) to only 4%mol EtOH dilution. While running lean with ϕ_{AF} = 0.6 provided the highest reactor section temperatures due to effects of oxidant preheat, ϕ_{AF} = 1.2 was the best operational condition tested as it exhibited the highest temperature increase based on the inlet temperature of the reagents. During oxidation

of 4%mol EtOH with air with ϕ_{AF} = 1.2 the reactor section was 36°C cooler than the case with H_2O_2, as a result of a change in overall fuel concentration (increased nitrogen content). While providing slightly lower reactor section temperatures, the use of air is recommended instead of H_2O_2 because of issues with pump reliability and practical application in the field. The cost of air is also 500% cheaper, not including the cost of damaged pumps operating with hydrogen peroxide. An additional reduction in cost can be achieved by replacing bottled air with an air compressor.

The fabrication of this SCWO reactor is just the start. Further testing with air at various fuel concentrations and reactor section TC locations will be required to gain additional knowledge of reactor parameters with air and to assist in CFD modeling. Additionally, the effects of a cooled wall via the external heat exchanger coiled around the reactor section and/or with sheath flow will likely be tested for corrosion and plugging mitigation. Destruction of CWA surrogates and other toxic compounds will be tested. Pending findings from these initial tests, a mobile reactor capable of filed operation will be designed.

REFERENCES

[1] D. Hoornweg, P. Bhada-Tata, and C. Kennedy, "Environment: Waste production must peak this century," *Nature News,* vol. 502, no. 7473, p. 615, 2013.

[2] D. Xu *et al.*, "Design of the first pilot scale plant of China for supercritical water oxidation of sewage sludge," *Chemical Engineering Research and Design,* vol. 90, no. 2, pp. 288-297, 2012, doi: 10.1016/j.cherd.2011.06.013.

[3] M. Svanström, M. Fröling, M. Modell, W. A. Peters, and J. Tester, "Environmental assessment of supercritical water oxidation of sewage sludge," *Resources, conservation and recycling,* vol. 41, no. 4, pp. 321-338, 2004.

[4] M. Goto, T. Nada, A. Kodama, and T. Hirose, "Kinetic analysis for destruction of municipal sewage sludge and alcohol distillery wastewater by supercritical water oxidation," *Industrial & engineering chemistry research,* vol. 38, no. 5, pp. 1863-1865, 1999.

[5] A. Gidner and L. Stenmark, "Supercritical water oxidation of sewage sludge–State of the art," in *Proceedings of the IBC's Conference on Sewage Sludge and Disposal Options*, 2001: Elsevier Karlskoga.

[6] D. A. Patterson, L. Stenmark, and F. Hogan, "Pilot-scale supercritical water oxidation of sewage sludge," in *Presented at the 6th European Biosolids and Organic Residuals Conference*, 2001, vol. 11, p. 14.

[7] T. Hübner, M. Roth, and F. Vogel, "Hydrothermal Oxidation of Fecal Sludge: Experimental Investigations and Kinetic Modeling," *Industrial & engineering chemistry research,* vol. 55, no. 46, p. 11910, 2016, doi: 10.1021/acs.iecr.6b03084.

[8] M. Cocero, "Supercritical Water Oxidation. Application to Industrial waste water treatment," *High Pressure Process Technology: Fundamentals and Applications. A. Bertuco, G. Vetter Eds. Elsevier,* 2000.

[9] S. Baur, H. Schmidt, A. Krämer, and J. Gerber, "The destruction of industrial aqueous waste containing biocides in supercritical water—development of the SUWOX process for the technical application," *The Journal of Supercritical Fluids,* vol. 33, no. 2, pp. 149-157, 2005.

[10] V. Vadillo, J. Sánchez-Oneto, J. R. Portela, and E. J. M. de la Ossa, "Supercritical water oxidation," in *Advanced Oxidation Processes for Waste Water Treatment*: Elsevier, 2018, pp. 333-358.

[11] J. Yang, S. Wang, Y. Li, Y. Zhang, and D. Xu, "Novel design concept for a commercial-scale plant for supercritical water oxidation of industrial and sewage sludge," *Journal of environmental management,* vol. 233, pp. 131-140, 2019.

[12] Y. Liu, C. Fan, H. Zhang, J. Zou, F. Zhou, and H. Jin, "The resource utilization of ABS plastic waste with subcritical and supercritical water treatment," *International Journal of Hydrogen Energy,* vol. 44, no. 30, pp. 15758-15765, 2019.

[13] M. Goto, M. Sasaki, and T. Hirose, "Reactions of polymers in supercritical fluids for chemical recycling of waste plastics," *Journal of Materials science,* vol. 41, no. 5, pp. 1509-1515, 2006.

[14] B. Bai, H. Jin, C. Fan, C. Cao, W. Wei, and W. Cao, "Experimental investigation on liquefaction of plastic waste to oil in supercritical water," *Waste management,* vol. 89, pp. 247-253, 2019.

[15] B. Bai, H. Jin, S. Zhu, P. Wu, C. Fan, and J. Sun, "Experimental investigation on in-situ hydrogenation induced gasification characteristics of acrylonitrile butadiene styrene (ABS) microplastics in supercritical water," *Fuel Processing Technology,* vol. 192, pp. 170-178, 2019.

[16] B. Bai *et al.*, "Experimental investigation on gasification characteristics of polycarbonate (PC) microplastics in supercritical water," *Journal of the Energy Institute,* vol. 93, no. 2, pp. 624-633, 2020.

[17] B. Bai *et al.*, "Experimental investigation on gasification characteristics of polyethylene terephthalate (PET) microplastics in supercritical water," *Fuel,* vol. 262, p. 116630, 2020.

[18] B. Bai, W. Wang, and H. Jin, "Experimental study on gasification performance of polypropylene (PP) plastics in supercritical water," *Energy,* vol. 191, p. 116527, 2020.

[19] Y. Shibasaki, T. Kamimori, J.-i. Kadokawa, B. Hatano, and H. Tagaya, "Decomposition reactions of plastic model compounds in sub-and supercritical water," *Polymer degradation and stability,* vol. 83, no. 3, pp. 481-485, 2004.

[20] D. Zou, Y. Chi, J. Dong, C. Fu, and M. Ni, "Supercritical water oxidation of MSW leachate: factor analysis and behavior of heavy metals," *Environmental Progress & Sustainable Energy,* vol. 33, no. 4, pp. 1117-1124, 2014.
[21] T. Mizuno, M. Goto, A. Kodama, and T. Hirose, "Supercritical water oxidation of a model municipal solid waste," *Industrial & engineering chemistry research,* vol. 39, no. 8, pp. 2807-2810, 2000.
[22] P. A. Marrone and G. T. Hong, "Corrosion control methods in supercritical water oxidation and gasification processes," *The Journal of Supercritical Fluids,* vol. 51, no. 2, pp. 83-103, 2009.
[23] C. Ludwig, S. Hellweg, and S. Stucki, *Municipal solid waste management: strategies and technologies for sustainable solutions*. Springer Science & Business Media, 2012.
[24] P. A. Marrone, S. D. Cantwell, and D. W. Dalton, "SCWO system designs for waste treatment: Application to chemical weapons destruction," *Industrial and Engineering Chemistry Research,* vol. 44, no. 24, pp. 9030-9039, 2005, doi: 10.1021/ie0506670.
[25] B. Veriansyah, J.-D. Kim, and J.-C. Lee, "Destruction of chemical agent simulants in a supercritical water oxidation bench-scale reactor," *Journal of hazardous materials,* vol. 147, no. 1-2, pp. 8-14, 2007. [Online]. Available: https://www.sciencedirect.com/science/article/abs/pii/S030438940601497X?via%3Dihub.
[26] T. Thomason, T. Thomason, and M. Modell, "Supercritical water destruction of aqueous wastes," *HAZARDOUS WASTE,* vol. 1, no. 4, pp. 453-467, 1984, doi: 10.1089/hzw.1984.1.453.
[27] *National Defense Authorization Act for Fiscal Year 1995,* U. S. o. America Act Pub.L. 103-337, 1994.
[28] M. L. Japas and E. Franck, "High pressure phase equilibria and PVT-data of the water-oxygen system including water-air to 673 K and 250 MPa," *Berichte der Bunsengesellschaft für physikalische Chemie,* vol. 89, no. 12, pp. 1268-1275, 1985.
[29] R. R. Steeper, S. F. Rice, M. S. Brown, and S. C. Johnston, "Methane and methanol diffusion flames in supercritical water," *The Journal of Supercritical Fluids,* vol. 5, no. 4, pp. 262-268, 1992, doi: 10.1016/0896-8446(92)90017-E.
[30] E. W. Lemmon, M. O. McLinden, and D. G. Friend, "Thermophysical Properties of Fluid Systems," in *NIST Chemistry WebBook, NIST Standard Reference Database Number 69*, vol. 20899, P. J. Linstrom and W. G. Mallard Eds. Gaithersburg MD: National Institute of Standards and Technology, ch. 20899.
[31] I. V. Novosselov, J. Kramlich, P. Reinhall, and D. Gorman, "Design and Validation of a Supercritical Water Gasification Reactor with In Situ Raman Spectroscopy for the Determination of Chemical Kinetic Rates," I. V. Novosselov, J. Kramlich, and P. Reinhall, Eds., ed: ProQuest Dissertations Publishing, 2018.
[32] R. M. Serikawa, T. Usui, T. Nishimura, H. Sato, S. Hamada, and H. Sekino, "Hydrothermal flames in supercritical water oxidation: investigation in a pilot scale continuous reactor," *Fuel,* vol. 81, no. 9, pp. 1147-1159, 2002, doi: 10.1016/S0016-2361(02)00015-7.
[33] M. C. Hicks, U. G. Hegde, and J. J. Kojima, "Hydrothermal ethanol flames in Co-flow jets," *The Journal of Supercritical Fluids,* vol. 145, pp. 192-200, 2019, doi: 10.1016/j.supflu.2018.12.010.
[34] M. D. Bermejo, D. Rincon, A. Martin, and M. J. Cocero, "Experimental performance and modeling of a new cooled-wall reactor for the supercritical water oxidation," *Industrial and Engineering Chemistry Research,* vol. 48, no. 13, pp. 6262-6272, 2009, doi: 10.1021/ie900054e.
[35] M. D. Bermejo, P. Cabeza, J. P. S. Queiroz, C. Jiménez, and M. J. Cocero, "Analysis of the scale up of a transpiring wall reactor with a hydrothermal flame as a heat source for the supercritical water oxidation," *The Journal of Supercritical Fluids,* vol. 56, no. 1, pp. 21-32, 2011, doi: 10.1016/j.supflu.2010.11.014.
[36] D. Zou, Y. Chi, C. Fu, J. Dong, F. Wang, and M. Ni, "Co-destruction of organic pollutants in municipal solid waste leachate and dioxins in fly ash under supercritical water using H2O2 as oxidant," *Journal of hazardous materials,* vol. 248, pp. 177-184, 2013.
[37] B. Wellig, K. Lieball, and P. R. von Rohr, "Operating characteristics of a transpiring-wall SCWO reactor with a hydrothermal flame as internal heat source," *The Journal of supercritical fluids,* vol. 34, no. 1, pp. 35-50, 2005.
[38] M. Modell, "Processing methods for the oxidation of organics in supercritical water," ed: Google Patents, 1982.

[39] Y.-L. Kim, J.-D. Kim, J. S. Lim, Y.-W. Lee, and S.-C. Yi, "Reaction pathway and kinetics for uncatalyzed partial oxidation of p-xylene in sub-and supercritical water," *Industrial & engineering chemistry research,* vol. 41, no. 23, pp. 5576-5583, 2002.
[40] P. Kritzer, "Corrosion in high-temperature and supercritical water and aqueous solutions: a review," *The Journal of Supercritical Fluids,* vol. 29, no. 1-2, pp. 1-29, 2004, doi: 10.1016/S0896-8446(03)00031-7.
[41] Z. Shen, L. Zhang, R. Tang, and Q. Zhang, "SCC susceptibility of type 316Ti stainless steel in supercritical water," *Journal of Nuclear Materials,* vol. 458, pp. 206-215, 2015.
[42] D. A. Hazlebeck, K. W. Downey, and M. H. Spritzer, "Downflow hydrothermal treatment," ed: Google Patents, 2000.
[43] P. Crooker, K. Ahluwalia, Z. Fan, and J. Prince, "Operating results from supercritical water oxidation plants," *Industrial & engineering chemistry research,* vol. 39, no. 12, pp. 4865-4870, 2000.
[44] B. R. Foy, K. Waldthausen, M. A. Sedillo, and S. J. Buelow, "Hydrothermal processing of chlorinated hydrocarbons in a titanium reactor," *Environmental science & technology,* vol. 30, no. 9, pp. 2790-2799, 1996.
[45] Y. Calzavara, C. Joussot-Dubien, H.-A. Turc, E. Fauvel, and S. Sarrade, "A new reactor concept for hydrothermal oxidation," *The Journal of supercritical fluids,* vol. 31, no. 2, pp. 195-206, 2004.
[46] N. R. Council, *Interim Design Assessment for the Blue Grass Chemical Agent Destruction Pilot Plant*. National Academies Press, 2005.
[47] M. Cocero and J. Martınez, "Cool wall reactor for supercritical water oxidation: modelling and operation results," *The Journal of supercritical fluids,* vol. 31, no. 1, pp. 41-55, 2004.
[48] P. A. Marrone, S. D. Cantwell, and D. W. Dalton, "SCWO system designs for waste treatment: application to chemical weapons destruction," *Industrial & engineering chemistry research,* vol. 44, no. 24, pp. 9030-9039, 2005.
[49] D. H. Xu, S. Z. Wang, Y. M. Gong, Y. Guo, X. Y. Tang, and H. H. Ma, "A novel concept reactor design for preventing salt deposition in supercritical water," *Chemical Engineering Research and Design,* vol. 88, no. 11, pp. 1515-1522, 2010.
[50] F. Zhang, C. Su, Z. Chen, and J. Chen, "Experimental study on the mixing characteristics inside an inner preheating transpiring-wall reactor for supercritical water oxidation," *The Journal of Supercritical Fluids,* vol. 156, p. 104682, 2020.
[51] B. R. Pinkard, A. L. Purohit, S. J. Moore, J. C. Kramlich, P. G. Reinhall, and I. V. Novosselov, "Partial Oxidation of Ethanol in Supercritical Water," *Industrial & Engineering Chemistry Research,* vol. 59, no. 21, pp. 9900-9911, 2020/05/27 2020, doi: 10.1021/acs.iecr.0c00945.
[52] S. Zhang *et al.*, "A Review of Challenges and Recent Progress in Supercritical Water Oxidation of Wastewater," vol. 204, ed, 2017, pp. 265-282.
[53] B. R. Pinkard *et al.*, "Supercritical water gasification: practical design strategies and operational challenges for lab-scale, continuous flow reactors," *Heliyon,* vol. 5, no. 2, p. e01269, 2019.
[54] R. K. Chakrabarty, I. V. Novosselov, N. D. Beres, H. Moosmüller, C. M. Sorensen, and C. B. Stipe, "Trapping and aerogelation of nanoparticles in negative gravity hydrocarbon flames," *Applied Physics Letters,* vol. 104, no. 24, p. 243103, 2014.
[55] J. Davis, K. Tiwari, and I. Novosselov, "Soot morphology and nanostructure in complex flame flow patterns via secondary particle surface growth," *Fuel,* vol. 245, pp. 447-457, 2019/06/01/ 2019, doi: https://doi.org/10.1016/j.fuel.2019.02.058.
[56] G. Mahamuni *et al.*, "Excitation-Emission Matrix Spectroscopy for Analysis of Chemical Composition of Combustion Generated Particulate Matter," *Environ Sci Technol,* Jun 1 2020, doi: 10.1021/acs.est.0c01110.
[57] J. Davis, E. Molnar, and I. Novosselov, "Nanostructure transition of young soot aggregates to mature soot aggregates in diluted diffusion flames," *Carbon,* vol. 159, pp. 255-265, 2020/04/15/ 2020, doi: https://doi.org/10.1016/j.carbon.2019.12.043.
[58] E. Molnar, "Effects of Temperature and Fuel Dilution on Soot Yields in an Inverted Gravity Flame Reactor," Master of Science in Engineering Master of Science in Engineering, Mechnical Engineering, Univiersity of Washington, Seattle, WA, 2019.
[59] J. Davis, "Characterization of combustion generated particulates produced in an inverted gravity flame reactor " Ph.D., University of Washington, Seattle, 2019.

[60] M. F. Karalus, K. B. Fackler, I. V. Novosselov, J. C. Kramlich, and P. C. Malte, "Characterizing the mechanism of lean blowout for a recirculation-stabilized premixed hydrogen flame," in *ASME Turbo Expo 2012: Turbine Technical Conference and Exposition*, 2012: American Society of Mechanical Engineers, pp. 21-30.
[61] K. B. Fackler, M. Karalus, I. Novosselov, J. Kramlich, P. Malte, and S. Vijlee, "NOx Behavior for Lean-Premixed Combustion of Alternative Gaseous Fuels," *Journal of Engineering for Gas Turbines and Power,* vol. 138, no. 4, p. 041504, 2016.
[62] Y. Guan and I. Novosselov, "EVALUATION OF LEAN BLOW-OUT MECHANISM IN TOROIDAL WELL STIRRED REACTOR," *Gas Turbine and Power,* vol. Submitted, 2017.
[63] A. Kaluri, P. Malte, and I. Novosselov, "Real-time prediction of lean blowout using chemical reactor network," *Fuel,* vol. 234, pp. 797-808, 2018/12/15/ 2018, doi: https://doi.org/10.1016/j.fuel.2018.07.065.
[64] S. Z. Vijlee, I. V. Novosselov, and J. C. Kramlich, "Effects of Composition on the Flame Stabilization of Alternative Aviation Fuels in a Toroidal Well Stirred Reactor," in *ASME Turbo Expo 2015: Turbine Technical Conference and Exposition*, 2015: American Society of Mechanical Engineers, pp. V003T03A007-V003T03A007.
[65] S. Gupta, P. Malte, S. L. Brunton, and I. Novosselov, "Prevention of lean flame blowout using a predictive chemical reactor network control," *Fuel,* vol. 236, pp. 583-588, 2019.
[66] C. Cui *et al.*, "Review on an advanced combustion technology: supercritical hydrothermal combustion," *Applied Sciences,* vol. 10, no. 5, p. 1645, 2020.
[67] C. R. Augustine, "Hydrothermal spallation drilling and advanced energy conversion technologies for engineered geothermal systems," Massachusetts Institute of Technology, 2009.
[68] S. Bianchetta, L. Li, and E. F. Gloyna, "Supercritical water oxidation of methylphosphonic acid," *Industrial and Engineering Chemistry Research,* vol. 38, no. 8, 1999, doi: 10.1021/ie990094p.
[69] E. Croiset, S. F. Rice, and R. G. Hanush, "Hydrogen peroxide decomposition in supercritical water," *Aiche journal,* vol. 43, no. 9, pp. 2343-2352, 1997.
[70] B. Pinkard, S. Shetty, J. Kramlich, P. G. Reinhall, and I. V. Novosselov, *Hydrolysis of Dimethyl Methylphosphonate (DMMP) in Hot-Compressed Water*. 2020.

A. APPENDIX

A.1 Standard Operating Procedure (SOP)

Procedures for Supercritical Water Oxidation Reactor (a.k.a. SCWOR, Hydrothermal Flame Reactor, or HFR) - High Temperature, High Pressure, Continuous Flow Apparatus with internal Combustion

Purpose and Scope:

This document describes the procedures and policies for using the ME department Supercritical Water Oxidation Reactor (a.k.a Hydrothermal Flame Reactor) located in MEB, B004. The reactor involves controlled chemical reactions of water, fuel, oxidants, and potentially hazardous chemicals, occurring at high temperatures (>300°C) and high pressures (>25 MPa). The scope of this document is to describe the operation of the reactor and establish user best practices. Instrument maintenance and repair are outside of the scope of this document.

Responsibilities:

This document is maintained by the Supercritical Water Reactor (SCWR) team, a part of the Novosselov Research Group (NRG). The SCWR group is responsible for general maintenance and for arranging repair when necessary. The SCWR group will operate the instruments according to the procedures in this document and will provide instruction and training to users within the department. Users are responsible for using the instrument described according to these procedures.

If you feel that the instrument needs repair or is not operating correctly, please notify:

Stuart Moore	–	stumoore@uw.edu	(509) 378-4070
Igor Novosselov	–	ivn@uw.edu	(206) 753-8447

Prerequisites:

All users must read this document and receive training from a trained team member currently within the supercritical water research group. Additionally, approval from one or more of the names listed above is needed prior to operating the reactor independently. Training will occur over three sessions of running the reactor under supervision, where users will learn how to:

- Operate and control the HPLC pumps
    - Prime the HPLC pumps (with possibly hazardous reagent)
- Operate Computer Programs
    - Thermocouple Readings (PICOLOG 6)
    - Solenoid Control
    - Air Mass Flow Controller (when applicable)
- Operate and ensure function of the heat exchanger
- Control internal reactor pressure
- Control internal reactor temperature using multiple PID controllers
- Collect data
    - Take Samples
    - Monitor and log thermocouple data (PICOLOG 6)
    - Monitor and log RAMAN data (when applicable)
- Troubleshoot common issues with the heaters, pumps and heat exchanger
- Empty the collection tank into appropriately labeled chemical waste containers
- Identify any potentially hazardous issues

- Ensure adequate ventilation and safe reactor operation

Users must also obtain standard EHS training on the use of fire extinguishers, the use of fume hoods, and managing laboratory chemicals.

Precautions and Hazards:

PPE - Use proper safety equipment and safety protocols when using the reactor. At a minimum, lab gloves, lab coat, and safety glasses should be worn when priming or handling hazardous reagents, or when handling reactor insulation. A dust mask should be worn when handling insulation. A respirator and lab coat should be worn when preparing hazardous reagents for use within the reactor. Closed toe shoes and long sleeves/pants should always be worn.

Chemical Hazards – Hazardous chemicals, (e.g. formic acid, methanol, DMMP) are frequently run through the reactor as reagents, and/or produced in the reactor as liquid or gaseous products (e.g. acetaldehyde, formaldehyde, CO). Always ensure adequate ventilation by closing the fume hood and making sure it is functioning properly. Wear proper PPE when priming reagents through the HPLC pump or when transporting reagents. Take steps to eliminate the possibility of exposure to hazardous fumes. Wear proper PPE when emptying the waste collection container.

Mechanical Hazards – The reactor can reach temperatures of 600C and internal temperatures of over 2000K can be present while also maintaining pressure of 0-30 MPa. The reactor tubing is small and could be compromised if struck. Be cautious due to fragility and note that all components are very expensive to replace. The heating elements are operated at extremely high temperatures and are dangerous to touch. Do not touch the reactor or pressurized components while it is running or under pressure. Components may be under high stress, and failure could be hazardous.

Do not attempt repair or service. If service is required, contact the lab manager immediately. Always ensure the polycarbonate safety panels are housing the reactor during operation. Never run heaters when pumps are shut off, as components could overheat. Always ensure that the heat exchanger system is running and functioning correctly before initializing the heaters. If the heat exchanger fails, immediately shut off the heaters and pumps and wait for the system to reach ambient temperatures.

In case of emergency turn off heaters and pumps immediately and then assess the situation and act accordingly.

Standard Operating Procedure:

Following is a step-by-step description of the general operating procedure for conducting experiments. Each process can be unique, and some steps may not be required.

1. Determine the type of process required before beginning. Determine the desired operating conditions including pressure, temperature, fuel and reagents to test, and proper flow rates.

2. Check that the reactor is available and fill out use log. Be sure to include all operation conditions listed above.

3. Prior to turning on reactor, visually inspect reactor to make sure it is operational. Ensure the safety shields are in place. Ensure the waste container is emptied.

Start Up

4. Turn on Computer and open the following programs:

i. PICOLOG 6 for thermocouple DAQ and begin recording and monitoring reactor temperatures
ii. Solenoid Control
iii. Sierra Mass Flow Control (when applicable/ running with Air)

5. Turn on the power strip to power up all components of the reactor

6. Program desired flow rates into HPLC pumps and begin running DI water through the system. IF RUNNING H2O, USE DI H2O ONLY. DO NOT USE TAP WATER. Ensure no Air in the pump lines. Prime pumps if needed.

6.1 Fuel pump – Before running, ensure the correct inlet lines from the solenoids are collecting from H2O and Fuel. H2O should be solenoid "closed or off" and fuel should be "open or on". Prime the lines if needed. Start running pump with H2O ensuring Solenoid Control program is set to "closed or off".

6.1.1 IF RUNNING PRE-MIX FUEL – Only 1 pump is needed for operation. Set desired flow rates for the pre-mix fuel on the pump labeled "fuel pump".

6.1.2 IF RUNNING PURE FUEL – Two pumps are needed. Set desired flow rates of pure fuel and necessary water diluent on their respective pumps. The water diluent pump will require no solenoid.

6.2 Oxidant pump

6.2.1. IF RUNNING H2O2 - Set desired flow rates for the oxidant on the pump labeled "oxidant pump". Before running, ensure the correct inlet lines from the solenoids are collecting from H2O and Hydrogen Peroxide. H2O should be solenoid "closed or off" and H2O2 should be "open or on". Prime the lines if needed. Start running pump with H2O ensuring Solenoid Control program is set to "closed or off".

6.2.2. IF RUNNING AIR – Oxidant pump should only be pulling from distilled water. H2O2 should not be hooked up to the system. Set flow rates for desired H2O flow rate. Set Sierra Mass Flow Control (MFC) computer program to "CLOSED" and ensure the valve to the system is closed. Open the Oxidant tank and ensure the Air tank pressure regulator output pressure is set to 4000 psig and that the tank pressure is >4500psig. Also note that if operating at 5 SLPM for 3 hours, approx. 500 psig of the tank will be consumed. Double check the valve of the Air line into the system is closed and set the desired flow rate for Air on the MFC control program and change the setting from "CLOSED" to "PRIME". When the program shows no flow through the MFC, change the setting from "PRIME" to "AUTO". DO NOT OPEN the valve into the system until after step 7.

7. Pressurize the system to the desired pressure using the back-pressure regulator (BPR). Note that the system will NOT pressurize immediately. Slowly apply pressure into the system by turning the BPR until resistance is felt and then waiting approximately 30 seconds- 3 min for the effects to be seen in the system as represented by the pressure readings on the pumps and the pressure gauge. After this initial pressurizing, there should no longer be a lag and the system can be slowly brought to desired pressure.

8. Allow the system to run at pressure for at least 5 minutes. Visually inspect the reactor again to ensure no leaks are present. If a leak is present, shut off the pumps, depressurize the system, and address the issue.

9. Initialize heat exchanger system and ensure proper function. If the system is not functioning correctly, shut off the pumps and depressurize the system and address the issue.

10. IF RUNNING AIR – Now that the system is pressurized, the valve on the Air line can be opened and closed as needed. The MFC program will stabilize flow at desired rates automatically. Note the calibration settings on the MFC require the inlet and outlet pressure of the MFC to be 4000 and 3600 psig respectively. After the valve is opened, double check the pressure gauge located immediately after the MFC to insure it reads 3600 psig during operation.

11. Slowly increase temperature for both oxidant and fuel by increasing heaters in 50C increments and waiting for the downstream TC to match (or plateau) temperature of the heater. (i.e. set heater to 100C, wait for TC reading to plateau at 95C, increase heaters to 150, etc.) Continue to do this until the desired operating temperatures have been reached.

12. Introduce oxidant into the system using the solenoid program on the computer, switching the oxidant solenoid from “CLOSED” to “OPEN”. Ensure there are no Air bubbles formed as this will require the pump to be re-primed. Monitor the temperature of the flow and adjust the temperature controller accordingly to get back to the desired flow rate.

> 12.1. To re-prime the pump during operation, the pump must be stopped. The valve located immediately after the pump outlet then needs to be switch to the “blocking flow” position to prevent loss of pressure of the reactor. At this point the pump can be primed and operation can resume. Ensure the prime dial is closed before re-opening the flow valve.

13. Introduce oxidant into the system using the solenoid program on the computer, switching the oxidant solenoid from “CLOSED” to “OPEN”. Ensure there are no Air bubbles formed as this will require the pump to be re-primed. Monitor the temperature of the flow and adjust the temperature controller accordingly to get back to the desired flow rate. *It is important to make sure the pump is primed before attempting to introduce fuel into the system. Do so in step 6 if needed. DO NOT RUN FUEL PRIOR TO OXIDANT

14. Monitor operation, noting that reactor wall temperature should never exceed 600C and fluid exit temperature should never exceed 30C (prevent scCO2 – this destroys back pressure regulator seals.

15. To quench, switch solenoid valves from “OPEN”, back to “CLOSED”. DO NOT change flow rates. Depending on flow rates, this may take a few minutes to observe.

FOR EMERGENCY SHUT OFF, TURN ALL PUMPS/ AIR LINES TO OFF. This should immediately extinguish operation. Wait a minute or two, switch solenoid valves to “CLOSED” to run water again and then flush with oxidant pump only for 5 minutes, then add fuel line pump with water. Running only oxidant pump at first ensures oxidant and fuel do not enter the system at the same time, reducing the likelihood for reignition due to residual fuel and oxidant in the lines.

Shut Down

16. Decrease set temperature on temperature controllers no more than 50°C at a time, to ensure system does not cool too rapidly, which could result in a leak. A good rule of thumb is to allow temperature in the fuel and oxidant lines to stabilize for at least 10 minutes before reducing temperature again. Increasing the flowrates could also cause rapid cooling and result in a leak. It is advised to maintain operating flow rates. Cool down from 400C should take at least 2 hours.

17. Monitor temperature in reactor. Once all temperatures (reactor and fluid) are below 100 C, depressurize system by slowly opening the back-pressure regulator.

18. Stop all pumps.

19. Switch pumps and heat exchanger to off. Turn off power supply(s). Save ALL data collected with notes clearly describing all changes in flow rates, inputs, errors, etc. This data should be saved with a easy to find name, follow naming procedure if it already exits.

Other

20. The product collection tank must be emptied periodically into appropriate chemical waste collection vessels. Use hazardous waste materials stickers to label the vessels appropriately. If more vessels are needed, contact the individuals identified above. If waste containers seem to be accumulating, contact UW EH&S for pick up:

https://ehs.washington.edu/chemical/hazardous-chemical-waste-disposal

21. Do not hesitate to ask questions.

Emergency Contacts and Procedures

Contacts:

911 – Life threatening emergency or accident, fire, explosion, hazardous material spill

(206) 543-0467 – EH&S Spill Line

(206) 685-1026 – Employee Health Clinic

(206)-684-8973 – UWPD non-emergency phone number (after hours contact)

If an accident occurs that is life threatening, call 911 immediately. If a minor accident occurs, it is recommended that the injured party go to Hall health and to fill out an accident report. Information can be found at: http://www.ehs.washington.edu/

Spill and Accident Procedures – In the case of a small chemical spill, use the spill kit and follow its directions to absorb chemicals. Use proper PPE (ventilator, gloves, lab coat, safety glasses). In the case of a large chemical spill, or the release of hazardous vapors, shut off the reactor heaters and pumps (power strips) and evacuate the lab. Contact the EH&S Spill Line (above) for assistance in spill cleanup. If chemical is spilled on yourself, use the eye wash or safety shower and remove contaminated clothing.

In case of Fire or Explosion – Activate the fire alarm and call 911. If the fire is small, use the nearest fire extinguisher to fight the fire. If the fire is large, evacuate the building immediately.

Chemical Storage and Disposal – Store chemicals in proper cabinets with clear labeling. DO NOT dump any chemicals down the drain. Use appropriately labeled hazardous waste containers to store waste chemicals and contact Environmental Health Services for disposal.

A.2 Supplementary Figures

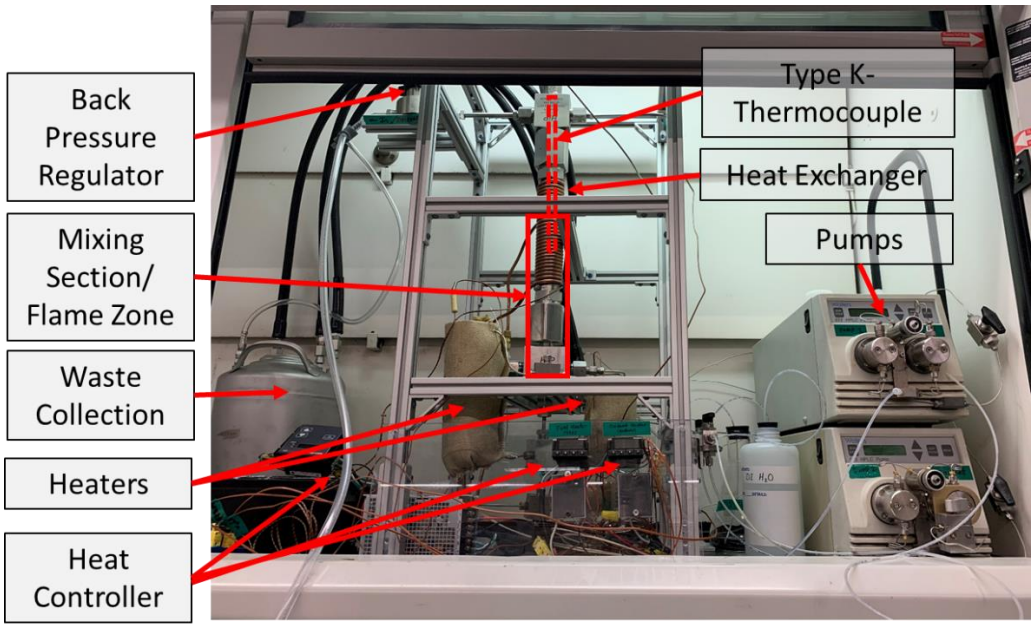

Figure S1: Design 2.1 in the upright confiuration.

Figure S2: Current Design 2.2 SCWO Reactor Design.

Figure S3: Shown here is the reactor with the Reactor Section TC (1”) located in the center, as outlined in Figure 11. This is the most recent observation of rust within the reactor section after running the hydrogen peroxide experiments presented in this thesis.